Environmental Laboratory

US Army Corps of Engineers®
Engineer Research and
Development Center
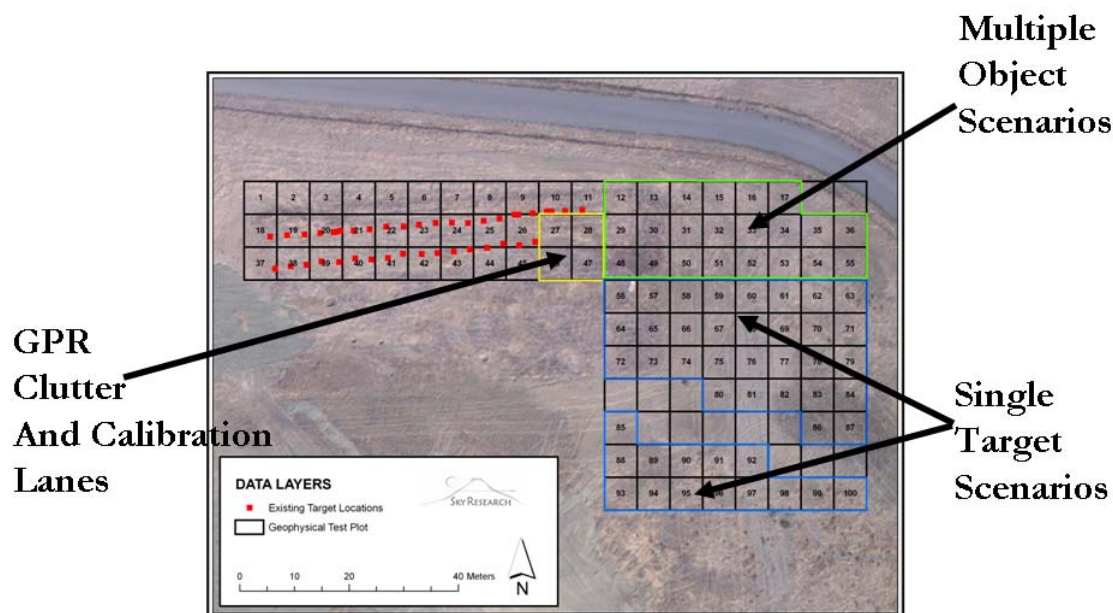
Environmental Quality and Installations Program

UXO Characterization: Comparing Cued Surveying to Standard Detection and Discrimination Approaches

Report 4 of 9
UXO Characterization Using Magnetic, Electromagnetic, and Ground Penetrating Radar Measurements at the Sky Research Test Plot

Stephen D. Billings, Leonard R. Pasion, Kevin Kingdon, and Jon Jacobson

September 2008

Multiple Object Scenarios

GPR Clutter And Calibration Lanes

Single Target Scenarios

DATA LAYERS
■ Existing Target Locations
☐ Geophysical Test Plot

SKY RESEARCH

0   10   20   40 Meters

N

UXO Characterization: Comparing Cued Surveying to Standard Detection and Discrimination Approaches

Report 4 of 9
UXO Characterization Using Magnetic, Electromagnetic, and Ground Penetrating Radar Measurements at the Sky Research Test Plot

Stephen D. Billings, Leonard R. Pasion, Kevin Kingdon, and Jon Jacobson

Sky Research, Inc.
445 Dead Indian Memorial Road
Ashland, OR 97520-9706

Report 4 of 9

Abstract: A test plot was established close to Sky Research's corporate headquarters in Ashland, OR. A comprehensive characterization of the site prior to emplacement of the ordnance was undertaken to gain an understanding of how the local soils would impact geophysical measurements. Conductivity and susceptibility measurements were made and soil samples were collected for laboratory analysis. Reconnaissance ground penetrating radar (GPR) surveys were conducted to investigate the penetration depths that could be expected and to characterize typical target responses. Penetration depths of approximately 1.0, 0.6, and 0.4 m were achieved using frequencies of 250, 500, and 1000 MHz, respectively. These measurements indicated that the Ashland test plot represented a challenging, yet realistic site in terms of its suitability for GPR measurements. The test plot was used to test modifications to equipment, new cued-interrogation strategies, and modeling methods. Data were collected with a wide range of sensors including time-domain electromagnetics (Geonics EM-61 and EM-63, the Zonge Bird-Cage), frequency-domain electromagnetics (Geophex GEM-3), total-field magnetometers (Geometrics cesium vapor G-823 sensors) and GPR (Sensors and Software Smart-Cart, Ohio State University fully polarmetric GPR). Various discrimination mode surveys including towed-array, cart-based, and man-portable, and cued-interrogation strategies were tested on the site.

Contents

Figures and Tables

Figures

Tables

Preface

Unit Conversion Factors

Multiply	By	To Obtain
feet	0.3048	meters

Acronyms

APG	Aberdeen Proving Ground
ATC	Aberdeen Test Center
A/D	analog-to-digital
cm	centimeter(s)
COTS	Commercial Off-the-Shelf
CRADA	Cooperative Research and Development Agreement
DAS	Data Acquisition System
DoD	Department of Defense
DSB	Defense Science Board
EM	Electromagnetic
EMI	Electromagnetic Induction
ERDC	Engineer Research and Development Center
FLBGR	Former Lowry Bombing and Gunnery Range
GPR	Ground Penetrating Radar
GPS	Global Positioning System
HEAT	High Explosive Anti-Tank
Hz	Hertz
IMU	Inertial Motion Unit
kHz	Kilohertz
m	meter(s)
MHz	Megahertz
mS/m	millisiemen per meter
ms	milliseconds
OSU	Ohio State University
RTK GPS	Real-time Kinematic Global Positioning System
RTS	Robotic Total Station
SERDP	Strategic Environmental Research and Development Program

SI	International System of Units
SNR	Signal-to-Noise Ratio
TEM	Transient Electromagnetic
UBC-GIF	University of Columbia's Geophysical Inversion Facility
UXO	Unexploded Ordnance
USACE	U.S. Army Corps of Engineers
YPG	Yuma Proving Ground
μs	microsecond(s)

General Introduction

The clearance of military facilities in the United States contaminated with unexploded ordnance (UXO) is one of the most significant environmental concerns facing the Department of Defense (DoD). A 2003 report by the Defense Science Board (DSB) on the topic estimated costs of remediation in the tens of billions of dollars. The DSB recognized that development of effective discrimination strategies to distinguish UXO from non-hazardous material is one essential technology area where the greatest cost saving to the DoD can be achieved.

The objective of project W912HZ-04-C-0039, "UXO Characterization: Comparison of Cued Surveying to Standard Detection and Standard Discrimination Approaches," was to research, develop, optimize, and evaluate the efficiencies of various modes of UXO characterization and remediation as a function of the density of UXO and associated clutter. Survey modes investigated in the research include:

1. Standard detection survey: All selected anomalies are excavated;
2. Advanced discrimination survey: Data collected in proximity to each identified anomaly are inverted for physics-based parameters and statistical or analytical classifiers are used to rank anomalies, from which a portion of the higher ranked anomalies are excavated;
3. Cued-survey mode: Each selected anomaly is revisited with an interrogation platform, high-quality data are collected and analyzed, and a decision is made as to whether to excavate the item, or whether to leave it in the ground.

Specific technical objectives of the research were to:

- Determine the feasibility and effectiveness of different interrogation approaches based on the cued-survey approach;
- Determine the feasibility and effectiveness of different interrogation sensors including magnetics, ground penetrating radar (GPR), and electromagnetic (EM) induction (EMI), and evaluate combinations of these sensors;
- Develop and evaluate the most promising interrogation platform designs;

- Develop optimal processing and inversion approaches for cued-interrogation platform data sets;
- Evaluate the data requirements to execute accurate target parameterization and assess the technical issues of meeting these requirements using detection and interrogation survey techniques;
- Determine which survey mode is most effective as a function of geological interference, and UXO/clutter density;
- Investigate the feasibility and effectiveness of using detailed test stand measurements on UXO and clutter to assist in the design of interrogation algorithms used in the cued-search mode.

The main areas of research involved in these coordinated activities include:

- Sensor phenomenology including GPR, EMI, and magnetometry;
- Data collection systems; platforms, field survey systems, field interrogation systems;
- Parameter estimation techniques; inversion techniques (single, cooperative, joint), forward-model parameterizations, processing strategies;
- Classification methods; thresholding, statistical models, information systems.

This report "UXO Characterization: Comparing Cued Surveying to Standard Detection and Discrimination Approaches: Report 4 of 9 – UXO Characterization Using Magnetic, Electromagnetic, and Ground Penetrating Radar Measurements at the Sky Research Test Plot," is one of a series of nine reports written as part of W912HZ-04-C-0039:

1. UXO Characterization: Comparing Cued Surveying to Standard Detection and Discrimination Approaches: Report 1 of 9 – Summary Report;
2. UXO Characterization: Comparing Cued Surveying to Standard Detection and Discrimination Approaches: Report 2 of 9 – Ground Penetrating Radar for Unexploded Ordnance Characterization; Fundamentals;
3. UXO Characterization: Comparing Cued Surveying to Standard Detection and Discrimination Approaches: Report 3 of 9 – Test Stand Magnetic and Electromagnetic Measurements of Unexploded Ordnance;
4. UXO Characterization: Comparing Cued Surveying to Standard Detection and Discrimination Approaches: Report 4 of 9 – UXO Characterization Using Magnetic, Electromagnetic, and Ground Penetrating Radar Measurements at the Sky Research Test Plot;

5. UXO Characterization: Comparing Cued Surveying to Standard Detection and Discrimination Approaches: Report 5 of 9 – Optimized Data Collection Platforms and Deployment Modes for Unexploded Ordnance Characterization;

6. UXO Characterization: Comparing Cued Surveying to Standard Detection and Discrimination Approaches: Report 6 of 9 – Advanced Electromagnetic and Magnetic Methods for Discrimination of Unexploded Ordnance;

7. UXO Characterization: Comparing Cued Surveying to Standard Detection and Discrimination Approaches: Report 7 of 9 – Marine Corps Base Camp Lejeune: UXO Characterization Using Ground Penetrating Radar;

8. UXO Characterization: Comparing Cued Surveying to Standard Detection and Discrimination Approaches: Report 8 of 9 – Marine Corps Base Camp Lejeune: UXO Characterization Using Magnetic and Electromagnetic Data;

9. UXO Characterization: Comparing Cued Surveying to Standard Detection and Discrimination Approaches: Report 9 of 9 – Former Lowry Bombing and Gunnery Range: Comparison of UXO Characterization Performance Using Area and Cued-interrogation Survey Modes.

1   Introduction

To rapidly test and evaluate modifications to equipment, new cued-interrogation strategies, and modeling methods, it was essential to establish a test plot close to Sky Research's corporate headquarters in Ashland, OR. A suitable site was found near the Ashland Municipal Airport, approximately 200 meters (m) from Sky Research's hangar, where all fabrication and systems engineering work were conducted. A comprehensive characterization of the site prior to emplacement of ordnance was undertaken to gain an understanding of how the local soils would impact geophysical measurements. To enable advanced discrimination methodologies to be benchmarked, many of the items that were emplaced in the test plot were previously characterized by electromagnetic (EM) and magnetic measurements at the Engineer Research and Development Center (ERDC) test stand in Vicksburg, MS.

This report is divided into two main sections: (1) activities involved with the creation and development of the Ashland test site, and (2) a chronological summary of test plot surveys. Detailed analysis and comparisons of the results are presented in other reports in this series. (This is Report 4 of the nine-report series.)

2   Site Characterization and Soil Sampling

A soils characterization program of the Ashland test plot was conducted during the period 24–28 January 2005. Surface soils and soils to a depth of approximately 1 mm were collected and characterized. Magnetic susceptibility was measured at the sample locations using the Bartington MK2 system at a frequency of 0.958 kilohertz (kHz) (D-Sensor). Figure 1 illustrates the variations in magnetic susceptibility over the test plot site, which varies from about 40 to 200×10^{-5} SI. This represents a relatively low variation in susceptibility.
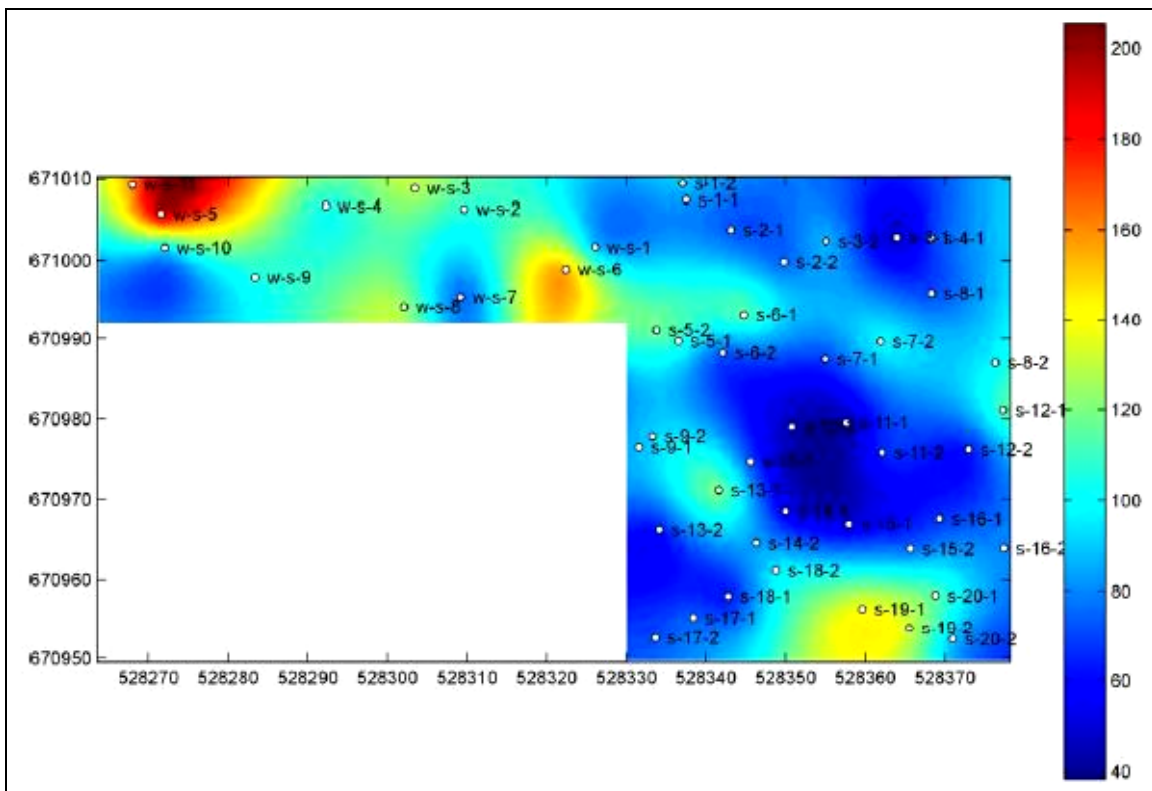
Figure 1. Magnetic susceptibility measurements (in units of 10^{-5} SI) of surface soils taken across the Ashland test plot site using the Bartington MK2 system. Surface soil sample locations are also labeled.

A conductivity survey of the site was conducted using a Geonics EM-38 system in the quadrature phase and held in a vertical position. Conductivity variations over the site are displayed in Figure 2. The linear band of conductivity in the lower half of the site is due to a buried steel pipe that traverses the area. Apart from that feature, there is little variation in soil conductivity across the site.
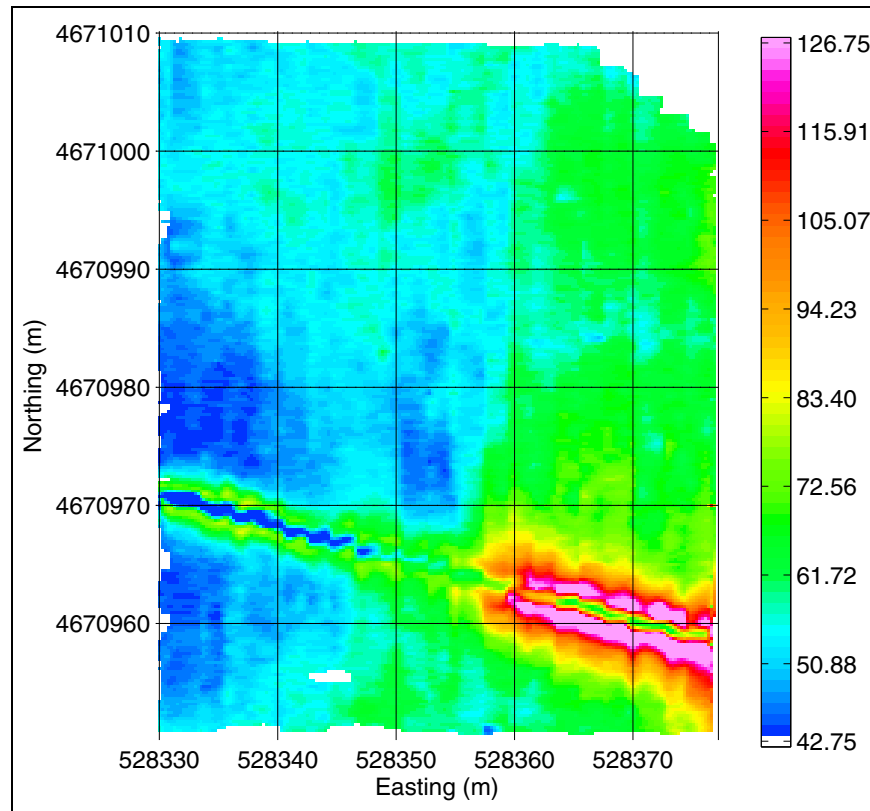
Figure 2. Electromagnetic conductivity measurements taken across the Ashland test plot site using a Geonics EM-38. Measurements are apparent conductivity in mS/m.

Fifty surface soil samples were collected in total at the site. The surface sample locations were chosen using randomly generated numbers and the samples were collected from the ground surface to a depth of 10 centimeters (cm). Eighteen of the 50 samples collected (surface and with depth) were chosen for laboratory analysis based on visual inspection and from results of EM and magnetics tests. The samples were submitted to the ERDC for analysis of water content, grain size distribution, mineral composition, and specific gravity. Two soil pits were dug at the site to characterize the soils with depth. Because of the limited variability in the surface soil visual characterization and magnetic susceptibility results, the locations of the two soil pits were chosen randomly. Test pits were advanced to a depth of approximately 1 m using a backhoe. Soil samples were taken at depths of 5, 30, 60, and 80 cm in each test pit. Further details on the Ashland site characterization and soil sampling can be found in the report *UXO Standardized Test Site: Soil Sampling Program, Ashland, Oregon* (Pasion et al. 2005).

2.1. Test plot GPR suitability surveys

During the same time period that soil sampling was undertaken at the site of the future test plot, GPR data were collected over two rows of previously emplaced items. The purpose of these surveys was to determine the performance of GPR. A commercial off-the-shelf (COTS) GPR system was chosen for these initial investigations for the robust and field-tested nature of the equipment and the ease of deployment and surveying. Equipment used for surveying at the Ashland test plot is shown in Figure 3. A comprehensive overview of the GPR results thus obtained is contained in Report 2: "UXO Characterization: Comparing Cued Surveying to Standard Detection and Discrimination Approaches: Ground Penetrating Radar for Unexploded Ordnance Characterization; Fundamentals" and, therefore, only an overview of test plot specific results will be presented here.

Figure 3. GPR surveying at the Ashland test plot with a 250-MHz system (upper left) and a 1000-MHz system (lower right).

Because the emplaced items were located in rows, a single GPR transect could be collected that incorporates responses from multiple targets. One such line of data is illustrated in Figure 4. Each of the targets produces a hyperbolic response as the GPR antenna moves over the target. Closely spaced pieces of shrapnel produce a combined response in the far right, as the resolution of the 250-megahertz (MHz) system is not sufficient to distinguish the separate items. The main goal of these initial GPR
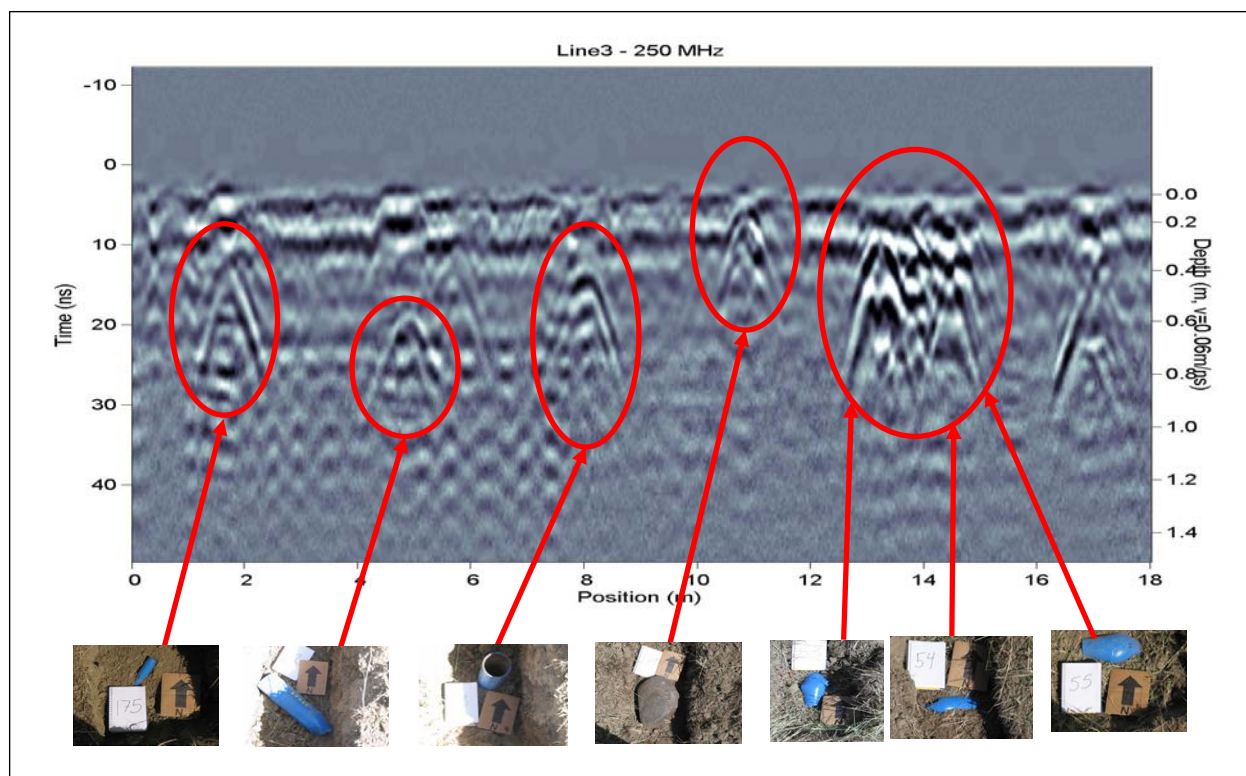
Figure 4. A single survey line collected with a 250-MHz GPR system. Target responses are indicated by red circles with photos taken at time of emplacement indicating the actual items.

surveys was to determine GPR suitability of the site, while a secondary goal was to develop a strategy for the deployment of a COTS GPR sensor as a cued-interrogation tool at future sites.

Measurements were also made over the same set of targets using a higher frequency 1000-MHz GPR system. Based on the data collected with the higher frequency system, individual responses were distinguished from the three distinct pieces of shrapnel that produced a combined response in the 250-MHz data. However, some of the deeper targets could no longer be detected using the 1000-MHz system, as the extra resolution is achieved at the expense of the penetration depth of the signal. This scenario is shown in Figure 5 where both 250-MHz and 1000-MHz data over the same targets are illustrated.

The Ashland test plot represented a challenging yet realistic site in terms of its suitability for GPR measurements. Penetration depths of approximately 1 m were achieved using a 250-MHz COTS GPR system. Using a higher frequency 1000-MHz system provided improved resolution,
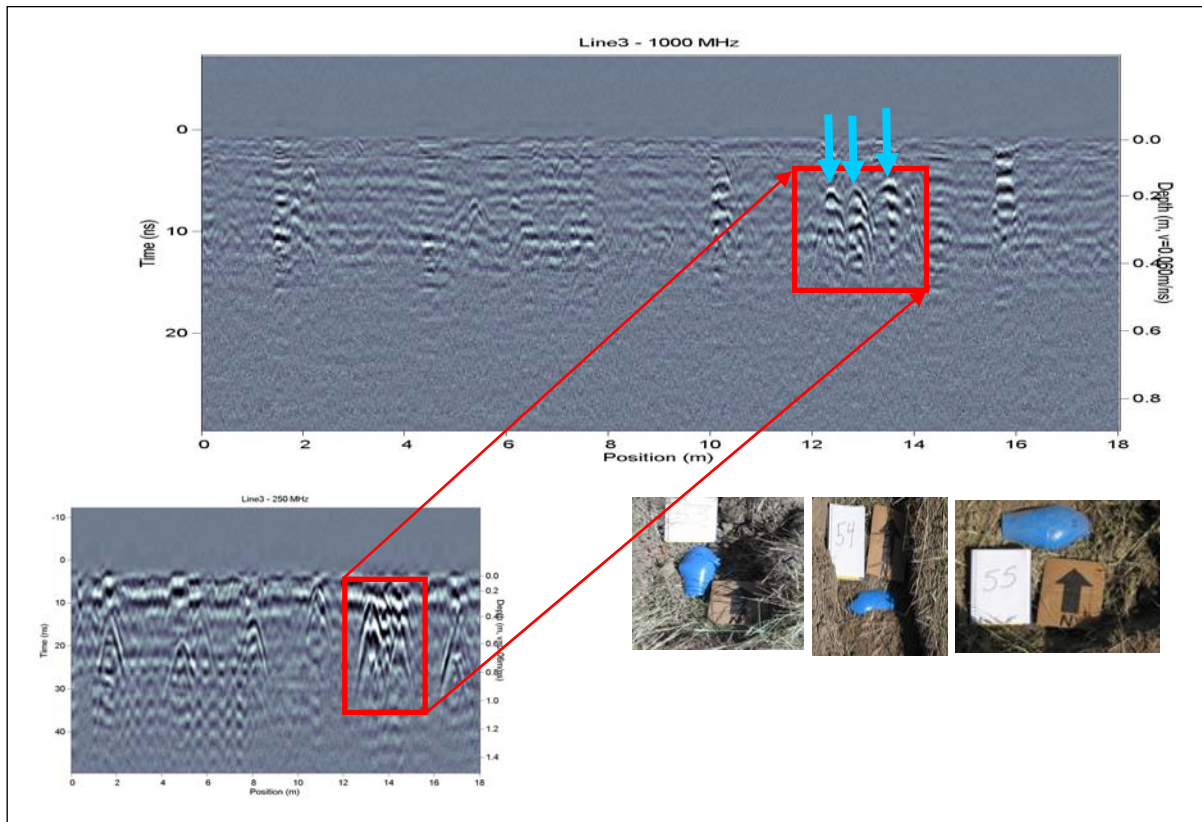
Figure 5. Using the higher frequency 1000-MHz GPR system permits the identification of three unique target responses corresponding to the three pieces of shrapnel that produced a single combined response in the 250-MHz data.

however, the penetration depth was limited to 0.4 m. The 500-MHz system was able to achieve a penetration depth of approximately 0.6 m. A second crucial consideration for the GPR suitability of a specific site is the presence of clutter. Because GPR technology relies on differences in electrical properties of host materials and targets, responses from non-metallic targets such as tree roots, cobble-sized rocks, soil horizons, and other geological features also are observed. Observations during the emplacement process indicated that substantial clutter was not present on the same order of size as UXO targets. There were, however, distinct soil horizons that respond similarly to clutter as they reflect some of the GPR signal back to the surface. Because these soil interfaces are horizontal, they generated flat-lying events in the GPR data and could be removed via background subtraction processing while the hyperbolic responses that are generated by the UXO targets were retained.

2.2. Test plot emplacement

Careful consideration was given to the Ashland test plot prior to emplacing items. A plan-view of the layout is shown in Figure 6. A number of cells were set aside for single target scenarios where emplaced items were placed far enough apart that a distinct response could be achieved with the geophysical sensors to be deployed. Single-object scenarios included a range of items from the Aberdeen Test Center (ATC) standardized reposi-tory (from 20- to 155-millimeter [mm] caliber) as well as some machined simulants and 76-, 81-, and 90-mm caliber items recovered from clearance work in Montana. The data collected from the ERDC test stand in Vicksburg, MS were used to determine the extent of the target responses for the various geophysical sensors.
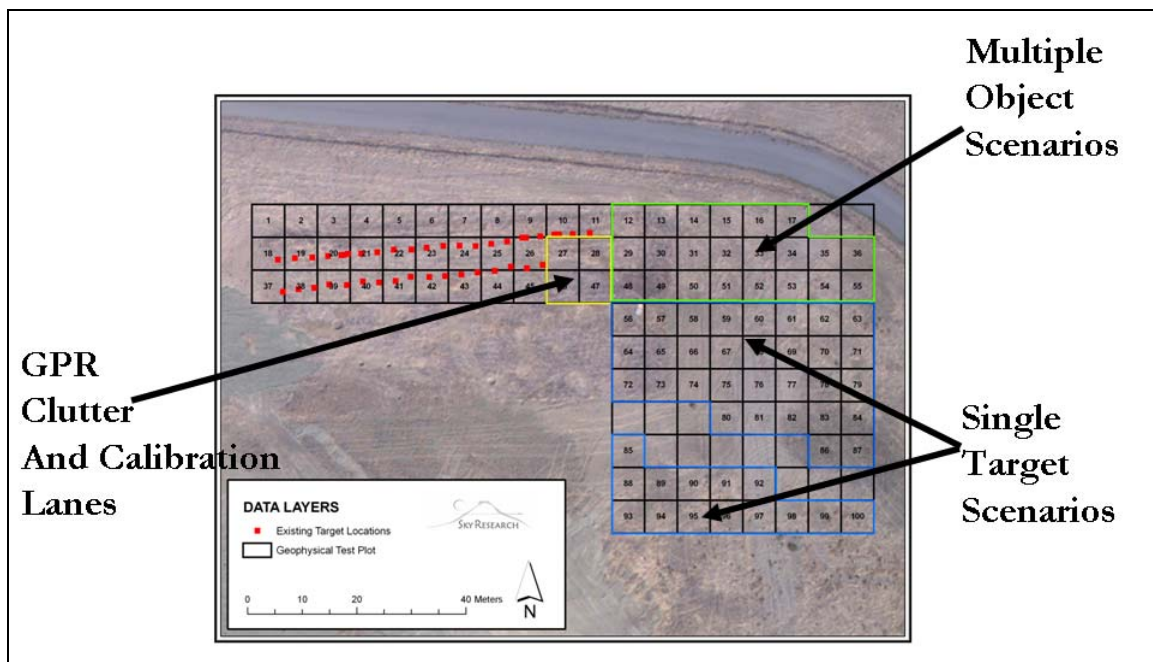
Figure 6. Layout of the Ashland test plot. Each cell measures 6 x 6 m.

Another section of the plot was designated the multi-object scenario section. In this region, more challenging target scenarios were created in order to test discrimination mode surveying in a complicated environ-ment. Targets were intentionally placed close enough such that the recorded signatures would overlap. Relatively large deeper targets were surrounded by shallow, small pieces of scrap. Certain cells were set aside to address specific problems. For example, 37-mm projectiles were sur-rounded by increasingly dense amounts of 20-mm shell casings to try and determine the best approach for identifying the 37-mm targets. A number

of cells were emplaced with GPR-specific clutter including tree roots, Styrofoam (to simulate voids), and large rocks. A detailed summary of emplaced items is available in Appendix B.

3   Chronological Summary of Test Plot Activities

Table 1 below provides a chronological summary of test plot activities, documenting the sensor type used, survey mode, and notes describing the specific activities performed.

Table 1. Summary of test plot activities

Date	Type	Mode	Comments
Jan. 05	EM-38, Bartington MK2, Soil Sampling	Site characterization	Conductivity measurements made over entire test plot. Magnetic susceptibility and soil samples collected at 50 locations
Jan. 05	Noggin 250 MHz, 1000 MHz GPR	Cued interrogation	Collection over targets both as single-pass profiles and as 2- by 2-m grid with 10-cm line spacing
June 05	NA	Target Emplacement	Targets were emplaced using combination of hand dug, backhoe, and auger
July 05	EM-63	Cued interrogation	Dynamic collection over four 1.8- by 1.8-m cells at 30-cm line spacing with standard cart
July 05	EM-63	Cued interrogation	Static collection over four 1.8- by 1.8-m cells at 30-cm station spacing, 30-cm line spacing with standard cart
July 05	EM-63	Cued interrogation	Static collection over ten 1.8- by 1.8-m cells at 30-cm station spacing, 30-cm line spacing on portable test stand
July 05	EM-63	Cued interrogation	Dynamic collection over one 1.8- by 1.8-m cell at 30-cm line spacing on portable test stand
July 05	GEM-3 (96 cm)	Cued interrogation	Dynamic collection over one 1.8- by 1.8-m cell at 30-cm line spacing with standard cart
July 05	GEM-3 (40 cm)	Cued interrogation	Static collection over four 1.8- by 1.8-m cells at 30-cm station spacing, 30-cm line spacing, two elevations on portable test stand
Sept. 05	EM-61	Detection	Full coverage of test plot at 0.5-m line spacing using gimbaled cart without inertial motion unit (IMU)
Sept. 05	EM-63	Detection	Full coverage of test plot at 0.5-m line spacing using standard cart without IMU
Sept. 05	Zonge birdcage	Cued interrogation	Static data collection over 14 cells
Jan. 06	EM-61	Discrimination	Gimbaled cart with IMU: System test prior to deployment to Aberdeen Proving Ground (APG)/Yuma Proving Ground (YPG)
Jan. 06	Magnetics	Discrimination	Man-portable array with IMU: System test prior to deployment to APG/YPG
Jan. 06	EM-61	Discrimination	Sky array with IMU: System test prior to deployment to APG/YPG

Date	Type	Mode	Comments
Feb. 06	EM-63	Cued interrogation	Dynamic collection over fifteen 1.8- by 1.8-m cells at 30-cm line spacing using suspension cart with IMU
Feb. 06	EM-63	Discrimination	Full coverage of test plot at 0.5-m line spacing using suspension cart with IMU
April 06	EM-61	Detection	Sky array without IMU: System test prior to deployment at Former Lowry Bombing and Gunnery Range (FLBGR)
April 06	EM-61	Discrimination	Sky array with IMU and a second prism on the rear left corner to test positional accuracy
May 06	Magnetics	Discrimination	Full coverage of test plot using the suspension cart with IMU in standard (4 sensors at 0.25-cm horizontal spacing) and gradiometer configurations (2- by 2-m sensors at 0.5-m horizontal, 0.5-m vertical spacing)
May 06	Magnetics	Discrimination	Full coverage of test plot using man-portable array with IMU
May 06	EM-61	Discrimination	Full coverage of test plot using suspension cart with RTS and EM-61 in three different modes: (i) Single receiver coil; (ii) Two receiver coils, top coil 14 cm above lower coil; and (iii) same as (ii) with top coil 28 cm above lower coil
June 06	Magnetics	Detection	Shakedown tests of the new Sky Research helicopter magnetometer system with cesium vapor magnetometer were conducted at various altitudes between 2 and 15 m
June 06	GEM-3 (40 cm)	Cued interrogation	Static collection over thirty-eight 1- by 1-m and 2- by 2-m cells at 20-cm station spacing, 20-cm line spacing using plywood template with holes drilled at appropriate station/line spacings
Sept. 06	OSU fully polarimetric GPR	Cued interrogation	Dynamic collection over 54 buried items at 3-in. station spacing. Two or three lines collected per target at a length of approximately 10 ft per line

3.1. Cued interrogation using EM-63 and GEM-3

During July 2005 data were collected using three instruments deployed in three survey modes. The goal of the data collection was to explore possible options for data collection in a cued-interrogation mode. The three systems tested were the Geonics EM-63, the GEM-3 96-cm head, and the GEM-3 40-cm head. In each survey mode the grid being interrogated was nominally 2 by 2 m. This scenario simulated the case where an individual target identified during a detection survey has been selected for follow-up using a cued-interrogation strategy. The three survey modes were wheeled dynamic, wheeled static, and test stand static. In the wheeled dynamic surveys, the large sensors (EM-63 and GEM-3 96-cm) were mounted on

wheeled carts. Wheeled dynamic mode data were collected along survey lines separated by 30 cm. The line locations were marked on a tarpaulin and the center of the tarpaulin was located over the target of interest (Figure 7).

Figure 7. Survey procedure used for wheeled static and dynamic surveys. The left photo shows the tarpaulin used for locating wheeled survey data. The right image shows the EM-63 during a wheeled survey.

During surveying, great care was taken to keep the sensor level with the ground surface and move slowly to ensure the greatest possible data fidelity. Positions were logged with the data using a real-time kinematic global positioning system (RTK GPS). In the static wheeled mode, data were collected at 30-cm intervals along the survey lines used in the dynamic mode. At each location, stationary data were collected for approximately 5 seconds. Positions were logged with the data using an RTK GPS. Test stand static data were collected on a semi man-portable test stand constructed from 8-ft 2×4 planks (see Figure 8).

The test stand was marked such that measurements over a 1.8- by 1.8-m grid could be collected at 10-cm spacing. The goal was to be able to collect data on a local grid with a high degree of repeatability. Local positioning was based on test stand coordinates. The corners of the test stand were measured using a robotic total station (RTS). All three sensors were deployed in this mode. Measurements with the large sensors were taken on a 30-cm grid covering the entire test stand. Measurements with the GEM-3 40-cm head were taken on a smaller 10-cm grid. The extents of the grid were defined for each target such that the anomaly was covered. Data were collected over 14 cells.

The results of this data collection effort were published in two papers in the *Journal of Applied Geophysics* (Pasion et al. 2007; Walker et al. 2007).

3.2. EM-61 and EM-63 standard cart GPS positioning

During September 2005 a small data collection campaign was carried out at the Ashland test plot. Data were collected along parallel transects spaced 0.5 m apart using the standard Geonics EM-61 and EM-63 carts (no suspension). Both systems were positioned using a GPS and no IMU was included. These surveys established the baseline detection and discrimination performance of the EM-61 and EM-63 prior to any modifications being made to the systems as part of this project. The data were processed using standard techniques including merging GPS and EM data, detrend filtering to remove instrument drift, etc. Images of the filtered data at time channels 1 (for the EM-63) and 3 (for the EM-61) are included in Appendix A. The performance metrics of the systems are compared to that of

Figure 8. Survey procedure for portable test stand measurements. The top image shows EM-63 measurements on the portable test stand. The bottom image is a close-up of GEM-3 measurements on the portable test stand. The positioning increments are visible in the bottom image.

the subsequently modified systems in Report 5: "UXO Characterization: Comparing Cued Surveying to Standard Detection and Discrimination Approaches: Optimized Data Collection Platforms and Deployment Modes for Unexploded Ordnance Characterization."

3.3. Zonge bird cage test

Zonge Engineering and Research acquired transient (time domain) electromagnetic (TEM) data over 14 Ashland test plot targets on September 21 and 22, 2005. An automated data acquisition system (DAS) was used in the development phase as part of Strategic Environmental Research and Development Program (SERDP) Project UX1309 to acquire multi-component TEM data for UXO target modeling and characterization. The goal of UX1309 is to improve "queued identification" by acquiring high-quality follow-up data over known target positions using a stationary TEM system.

Zonge Engineering's static TEM system has been nicknamed the "bird cage" for the appearance of its loop array (Figure 9). It uses three separate transmitter loops in sequence to illuminate the target object from three nearly orthogonal directions. A laptop computer runs an automated sequence controlling both a multiplexing system to select transmitter and receiver loop combinations and data acquisition by a Zonge Engineering ZT30 transmitter and GDP32 geophysical receiver. Novel features of the system include automated control of transmitter and receiver loop combinations with a loop multiplexing system and 24-bit A/D data acquisition for better resolution of small late-time TEM signals.
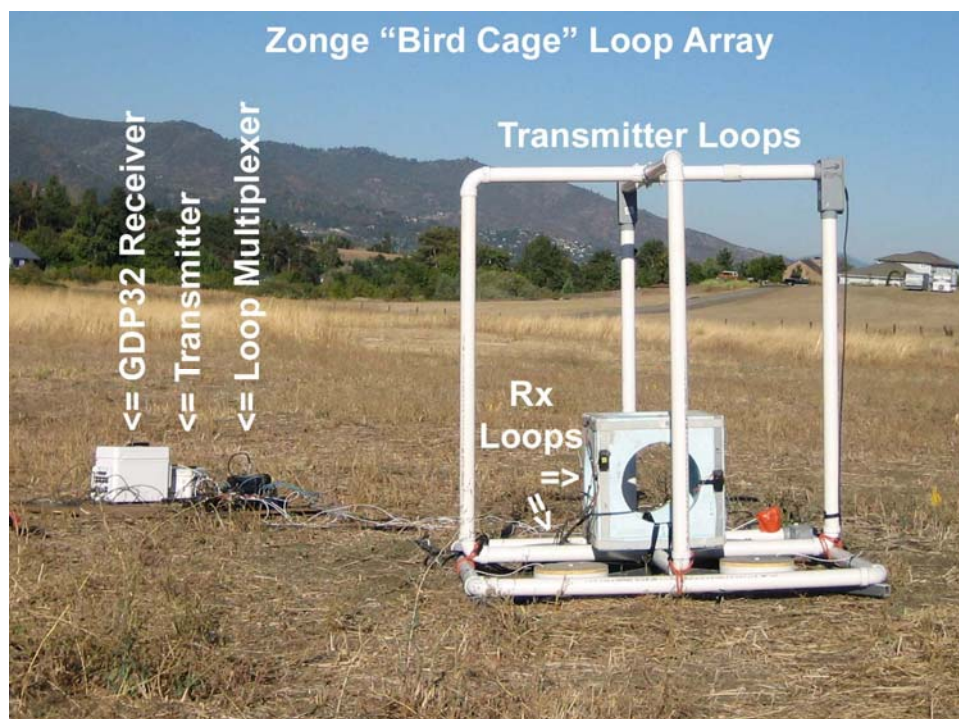
Figure 9. Zonge Engineering's bird cage follow-up TEM loop array.

The Zonge bird cage TEM system steps through a measurement sequence using each of its three transmitter loops in turn. First, the vertical loop with an east-west axis is used to illuminate the target object with an east-west source field, while making measurements with six receiver loops with good coupling to the target's primary response (Figure 10, left panel). Then, the second vertical loop is used to illuminate the target in the north-south direction (Figure 10, middle panel), again measuring the target's response with six well-coupled receiver loops. Finally, a horizontal transmitter loop illuminates the target object with a vertical source field (Figure 10, right panel) while transients for six vertical component receiver loops are recorded.
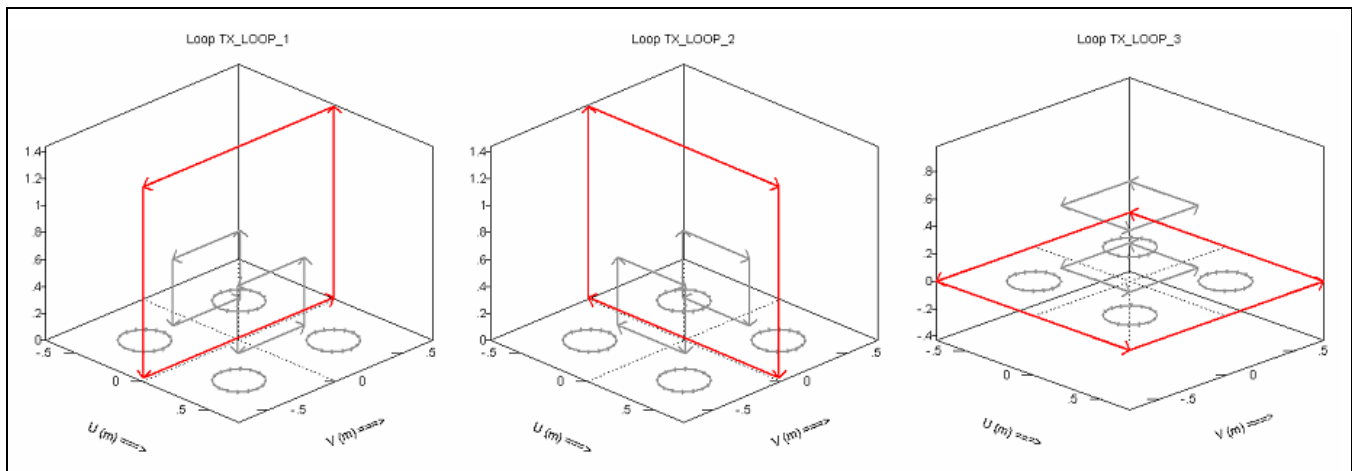
Figure 10. TEM measurement sequence illuminating the target object from three nearly orthogonal directions with source fields from three different transmitter loops, while monitoring the target's response with arrays of six receiver loops.

For each transmitter loop, time-series data are recorded for 128 or more cycles of a bipolar, rectangular pulse waveform (Figure 11). The inductive response of the target object is recorded after each transmitter current pulse, while the transmitter current is zero, to allow maximum sensitivity to the weak and rapidly decaying secondary magnetic field signal from currents induced in conductive targets. Receiver loop voltages are sampled at 32 kHz using 24-bit analog-to-digital conversion. The time-series data stream can either be saved as is for post-acquisition processing on an external computer or stacked, rectified, and binned to 28 sample TEM transients by the GDP32 receiver itself.

Tx Current and dB/dt EMF
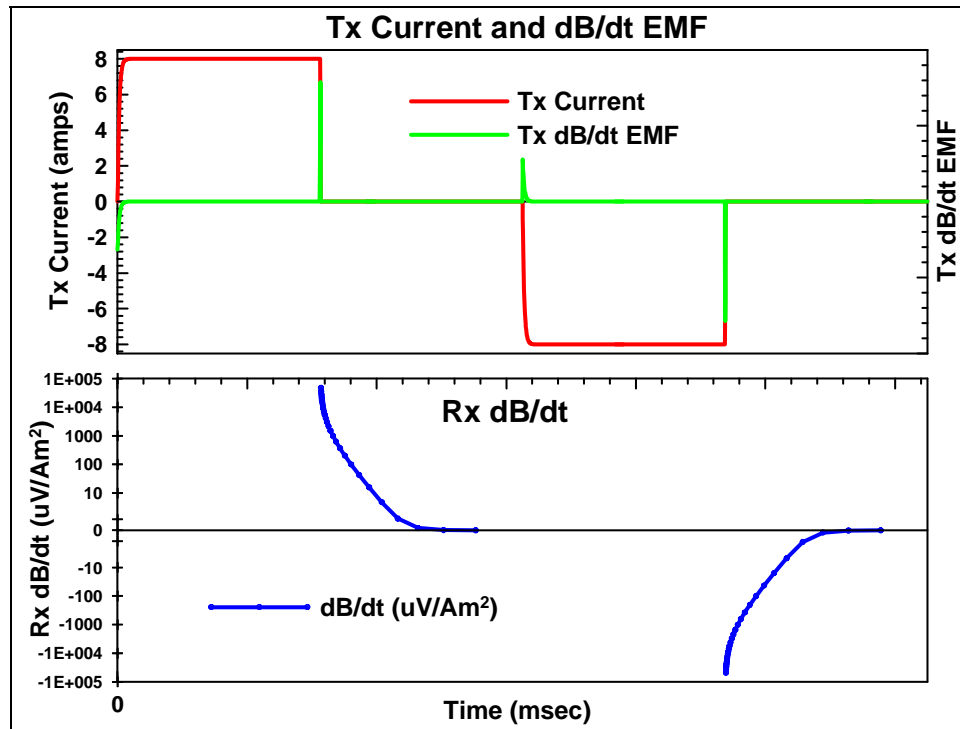
Figure 11. A bipolar rectangular pulse current waveform is used to generate source fields (red line in upper panel). The time-varying magnetic source field generated by transmitter waveform currents creates inductive pulses in nearby conductive targets (green line in upper panel). Secondary magnetic fields from any inducted currents produce transient voltages in the TEM system's receiver loops (lower panel).

Transients from six receiver loops are recorded for each transmitter loop. Each transient includes 28 time windows spaced logarithmically from 50 microseconds (μs) to 25 milliseconds (ms). Two complete measurement sequences are made for each target, one with the loop array displaced 2 m away from the target anomaly in order to measure nearby background, and a second with the loop array centered on the target anomaly to measure target response plus background. The background measurements are subtracted to obtain residual measurements of the target's TEM response. Figure 12 shows the six residual transients for z-directed source-field illumination of a 60-mm M493A buried at a depth of 17 cm in Ashland test plot Cell 73B.
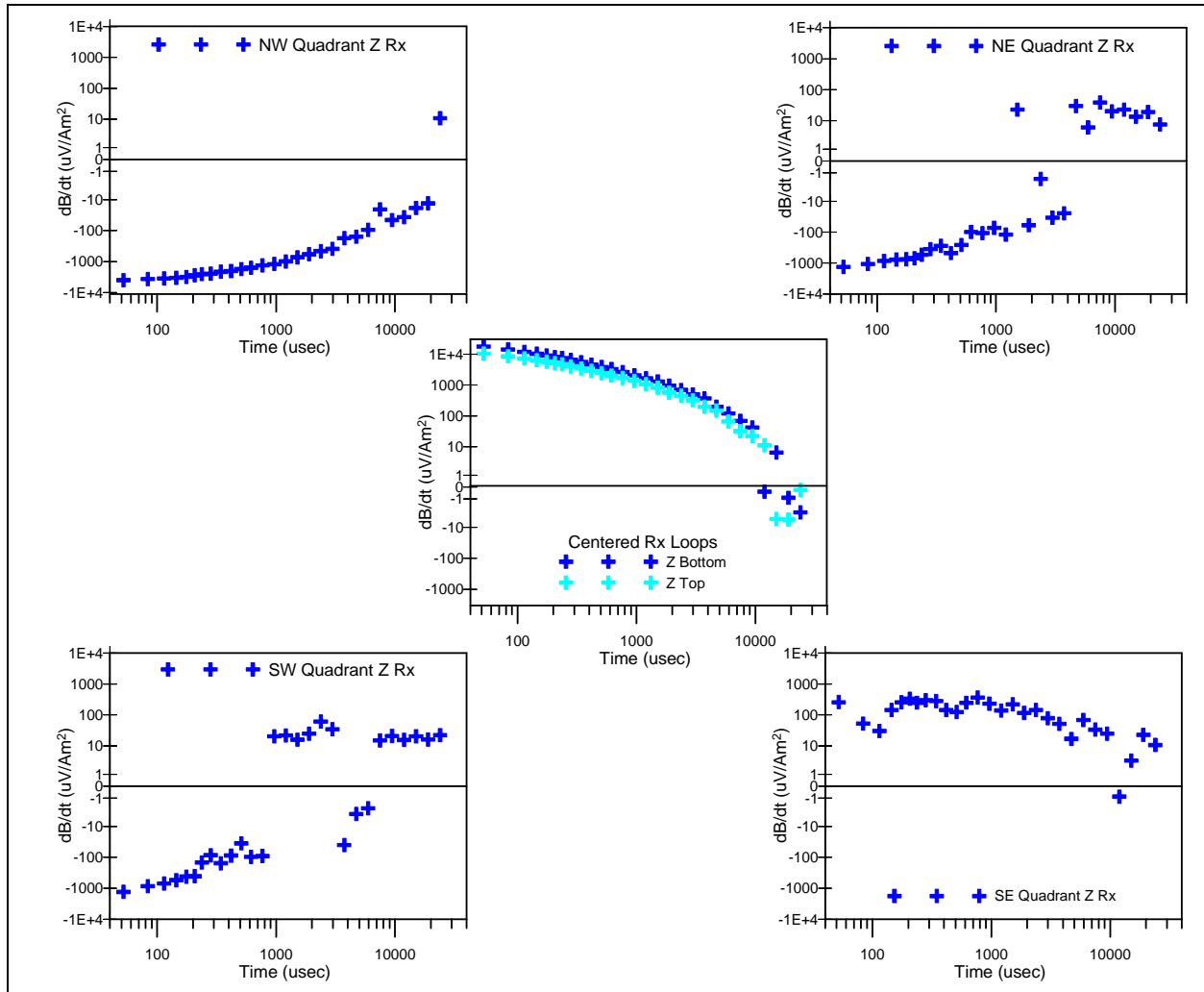
Figure 12. Secondary transients from the six vertical component receiver loops used to measure the target response during illumination with the z-directed transmitter loop. Residual data (with the background response subtracted out) are shown for measurements over a 60-mm M493A in Ashland test plot Cell 73B.

Residual TEM data are inverted to estimate polarizability transients along the three axes of spherical, spheroidal, and ellipsoidal target models (Figure 13), with the shape of each target axis polarizability transient characterized by the four-parameter Pasion-Oldenburg model

$$\frac{dP}{dt}(pk, pa, pb, pc) = \frac{pk \cdot \exp\left(-pc \cdot 10^{-3} \cdot t_{u\sec}\right)}{\left(pa + t_{u\sec}\right)^{pb}}$$

The system, as deployed in Ashland, was still in the experimental stage, but there were plans to make it field-ready within a year. Unfortunately, it was not ready in time for the cued-interrogation work at the FLBGR and Camp Lejeune field sites.
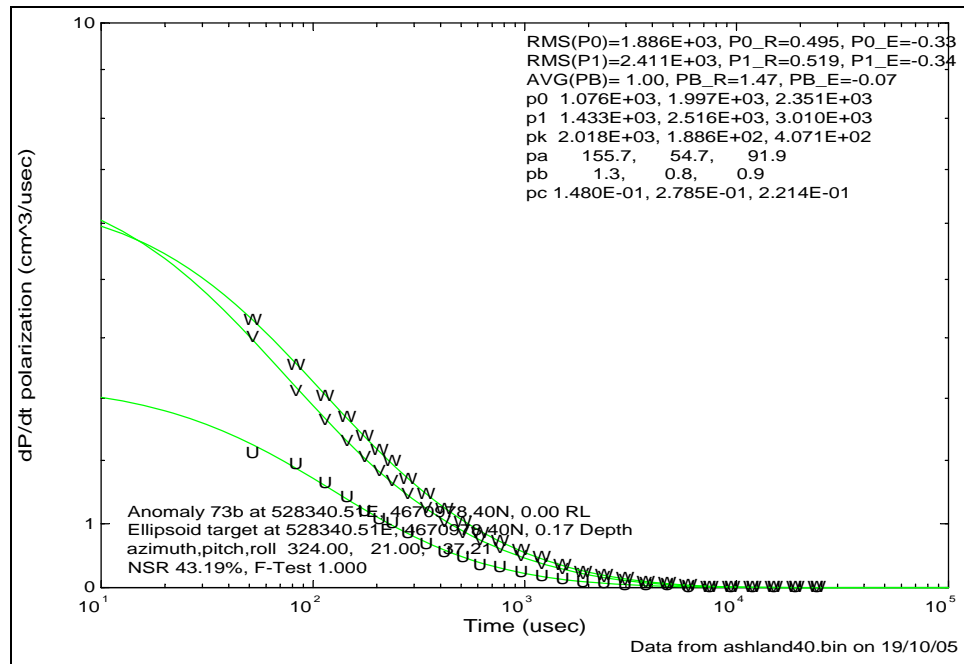
Figure 13. Target polarizability transients from inversion of follow-up TEM data over
a 60-mm M493A in Ashland test plot Cell 73.

3.4. Magnetometer array and EM-61 Cart with IMU

During 2005, modifications were made to many of the survey platforms
deployed by Sky Research (see Report 5). A significant improvement was
the addition of an IMU, which provides information on the pitch, roll, and
azimuth of a given sensor. In January 2006, a series of data sets were
collected over the Ashland test plot with the IMU and robotic total station
(RTS) for positioning. Images are not provided of these data sets here, as
subsequently additional improvements were made to the systems and
additional magnetometer and EM-61 data were collected in April/May
2006.

3.5. EM-63 suspension cart full coverage and cued interrogation

As discussed in Report 5, a number of modifications were made to the
EM-63 including incorporation of an IMU and the RTS and construction
of a new cart. The new cart is lower to the ground than the standard
EM-63 setup to increase the signal-to-noise ratio (SNR). The new cart also
has suspension to reduce sudden changes in orientation due to surveying
on uneven terrain. In addition to form factor modifications, the EM-63
was integrated with the Sky Research DAS. By using the RTS and IMU,
better estimates were extracted of the location, pitch, roll, and heading of
the coil at each measurement.

A photograph of the cart in action collecting discrimination mode data on the Ashland test plot is shown in Figure 14. An image of the first time-channel of discrimination mode data collected over the entire test plot is provided in Appendix A. Figure 15 shows cued-interrogation data over two cells; one contains a single object, while the other contains multiple objects. Additional cued-interrogation data acquired with this configuration of the EM-63 are available in Appendix A. Data quality from this new sensor system has been excellent, and the data are expected to have good discrimination capability.

Figure 14. Modified EM-63 cart collecting discrimination mode data at the Ashland test site.

3.6. EM-61 suspension cart with IMU full coverage

The EM-61 can use information in the top coil to resolve the depth to a buried item. This information may help remove some of the ambiguity inherent when trying to resolve the dipole parameters from a coil at one height. The objective of the measurements conducted in May 2006 was to determine if improved depth resolution of the top/bottom coil combination translates to improved discrimination performance (through better
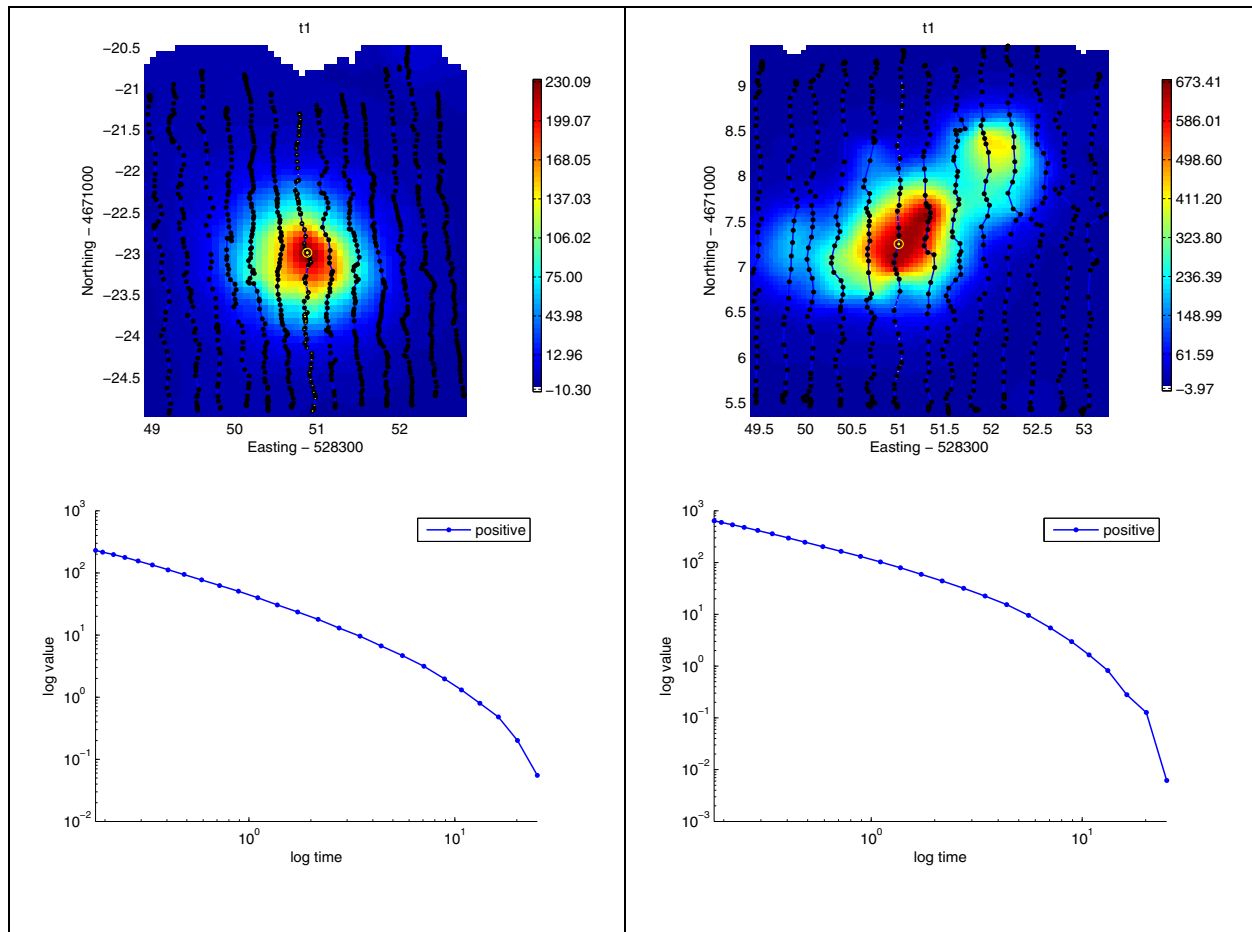
Figure 15. Examples of EM-63 cued-interrogation data collected on the Ashland test plot (gridded images of time-channel 1 and decay at the marked sounding near the center of the area covered). Target on the left is a single-object scenario comprising a horizontal 155-mm projectile at 35-cm depth. Target on the right is a multi-object scenario with a horizontal 105-mm projectile at 29-cm depth adjacent to two pieces of shrapnel. All units are in millivolts (mV).

estimates of the polarization tensor). The surveys were conducted to support a Cooperative Research and Development Agreement (CRADA) with USACE-Huntsville and used three different coil configurations (see Figure 16):

- Standard EM-61 measuring four channels in the bottom coil;
- Standard EM-61 (with top coil 30 cm above bottom) measuring three channels in the bottom coil and one in the top; and
- Modified EM-61 (with top coil 18 cm above bottom) measuring three channels in the bottom coil and one in the top.

Figure 16. EM-61 deployed in differential survey mode with the top coil mounted 16 cm above (left) and 30 cm above (right) the bottom coil.

Data were collected over the entire test plot with an EM-61 sensor mounted on a hydraulic cart. The RTS was used for positioning, and the Crossbow IMU was used for sensor orientation and to provide corrections to the RTS position based on the cart orientation. Standard calibrations (static, spike, cable-shake, time-slew, etc.) were conducted for each sensor system. The instrument was deployed in three different configurations. The data were merged together and a 151-point demedian filter was used to correct for temporal and spatial changes in the EM background. Images of these minimally processed data are shown in Appendix A. Additional details on the interpretation of these EM-61 data sets are provided in Billings et al. (2006), which was the document submitted for the Huntsville CRADA work.

3.7. Magnetometer array with RTS/IMU

Three different configuration magnetometer surveys were conducted at the Ashland test plot in May 2006 as part of the CRADA with USACE-Huntsville. The first was a cart-based quad-sensor array configured with 0.25-m sensor spacing 0.25 m above the ground (Figure 17). The second survey used a gradiometer configuration with two lower sensors 0.25 m above the ground at 50-cm spacing and two upper sensors 50 cm directly above the lower sensors. The third survey was with the man-portable quad-sensor array (see Figure 18, which shows the system in operation at FLBGR) configured with the sensors 37.5 cm apart. The operator carried the frame so the sensors were about 40 cm above the ground.

Figure 17. Magnetometer cart with sensors deployed at 25-cm elevation and 25-cm sensor separation. For the gradient configuration, the same cart was used with the upper sensors 50 cm above the lower ones.

Figure 18. Sky man-portable MAG array integrates four Geometrics G-823 with the Leica 360° prism and a Crossbow IMU for orientation.

Each of the surveys used the same Geometrics G823 cesium vapor total field magnetometers. A reference magnetometer was set up in a static location and used to record temporal changes in the Earth's magnetic field. All three systems were positioned with a Leica TPS 1206 RTS augmented by a Crossbow AHRS 400 IMU. By knowing the geometry of each sensor relative to the RTS prism, and the pitch and roll from the IMU, each sensor was precisely positioned in three dimensions.

A standard set of calibration tests were conducted before each survey including:

- Magnetometer/RTS time-slew test;
- IMU/RTS time-slew test; and
- Magnetometer octant test.

Magnetometer, RTS, and IMU data were merged together and heading and base-station corrections were applied. For the gradiometer, the processed data comprised both the magnetometer readings at each data as well as the difference between each upper and lower sensor pair (to approximate a gradiometer). Long-wavelength variations in the total-field and gradient data were removed using a 15-m-long demedian filter. The resulting data images are shown in Appendix A. Additional information on these magnetometer surveys can be found in Billings et al. (2006).

3.8. GEM-3 cued interrogation

During the period June 12–23, 2006, GEM-3 cued-interrogation surveys were completed over 38 targets on the Sky Research test plot in Ashland. The cells of the test plot that were surveyed are shown in Figure 19. The plan was to cover a variety of targets to highlight the strengths and weaknesses of the GEM-3. The cells highlighted with the green polygon contain small and medium ordnance items (20-mm projectile, 37-mm projectile, 40-mm grenade, M42 submunition, BLU-26 submunition, BDU-28 submunition, MK118 Rockeye and 60-mm mortar); the cells highlighted with the yellow polygon contain 105-mm High Explosive Anti-Tank (HEAT) rounds, and the cells highlighted with the pink polygon contain a series of multiple-object scenarios. Each multi-object cell contained 37-mm projectiles surrounded by an increasing density of 20-mm projectiles. The data over the small and medium size
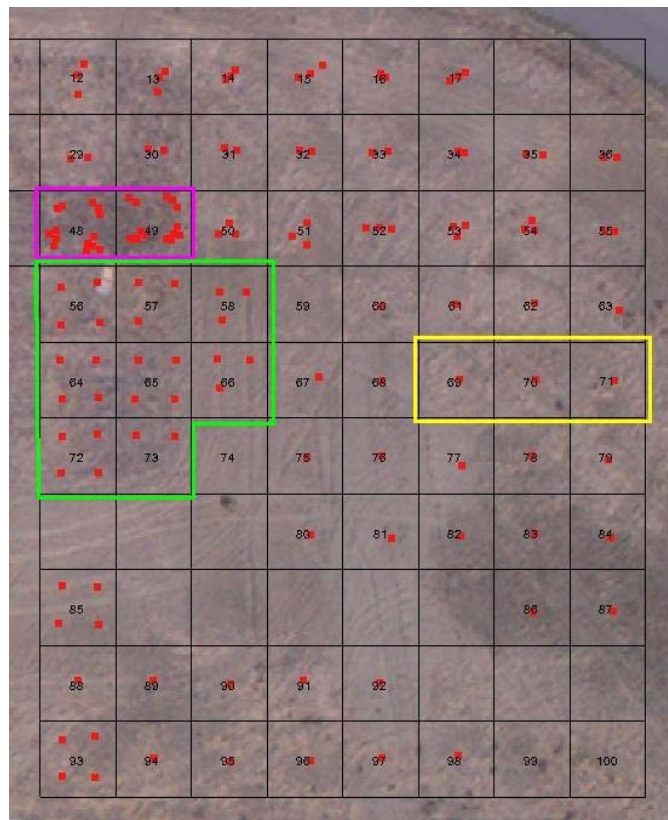
Figure 19. Plan showing the cells of Sky Research test plot that were surveyed using the GEM-3 in June 2006. Green polygon indicates cells surveyed that contain small and medium ordnance items, pink polygon indicates cells surveyed that contain multiple objects, and the yellow polygon indicates cells surveyed that contain 105-mm HEAT rounds.

targets were collected using the same 1- by 1-m template used at FLBGR. In order to cover the larger anomalies associated with the 105-mm HEAT rounds and the multi-object anomalies, data had to be collected over a 2- by 2-m area. This was accomplished by surveying four different 1- by 1-m areas with a uniform grid of 36 points with 20-cm station separation. Each of the four segments represented a quadrant of the final survey area as shown by the schematic in Figure 20. To ensure complete coverage, the edges of the four surveys overlapped.
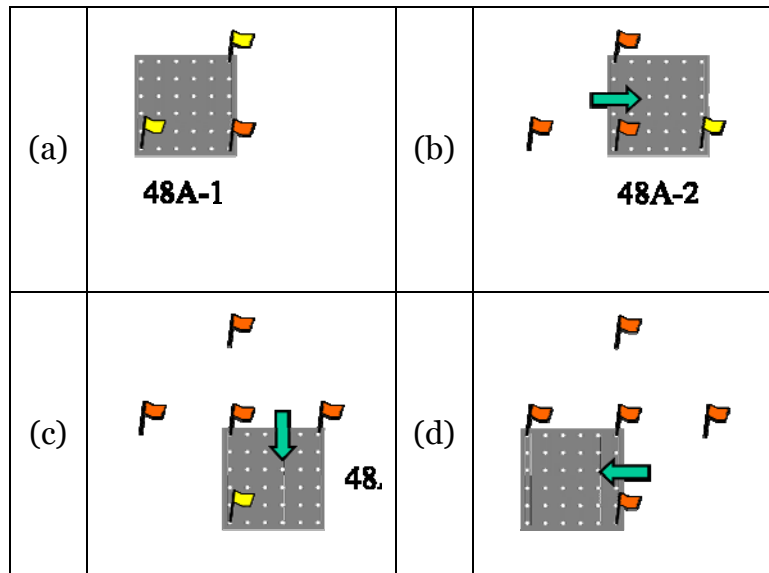
Figure 20. Schematic of the survey procedure for large targets and multi-object cells using a 1- by 1-m template. In each panel the orange pin flags represent flags that have been placed in the ground to locate the template. The yellow pin flags represent new flags that are placed in the ground and will be used during subsequent surveys. The green arrows indicate the direction the template has been moved.

Data from two targets are shown in Figure 21. The first target is a 20-mm projectile (small ferrous item); the second target is a 40-mm grenade (small non-ferrous item). The depth and orientation of each item are shown in Table 2.
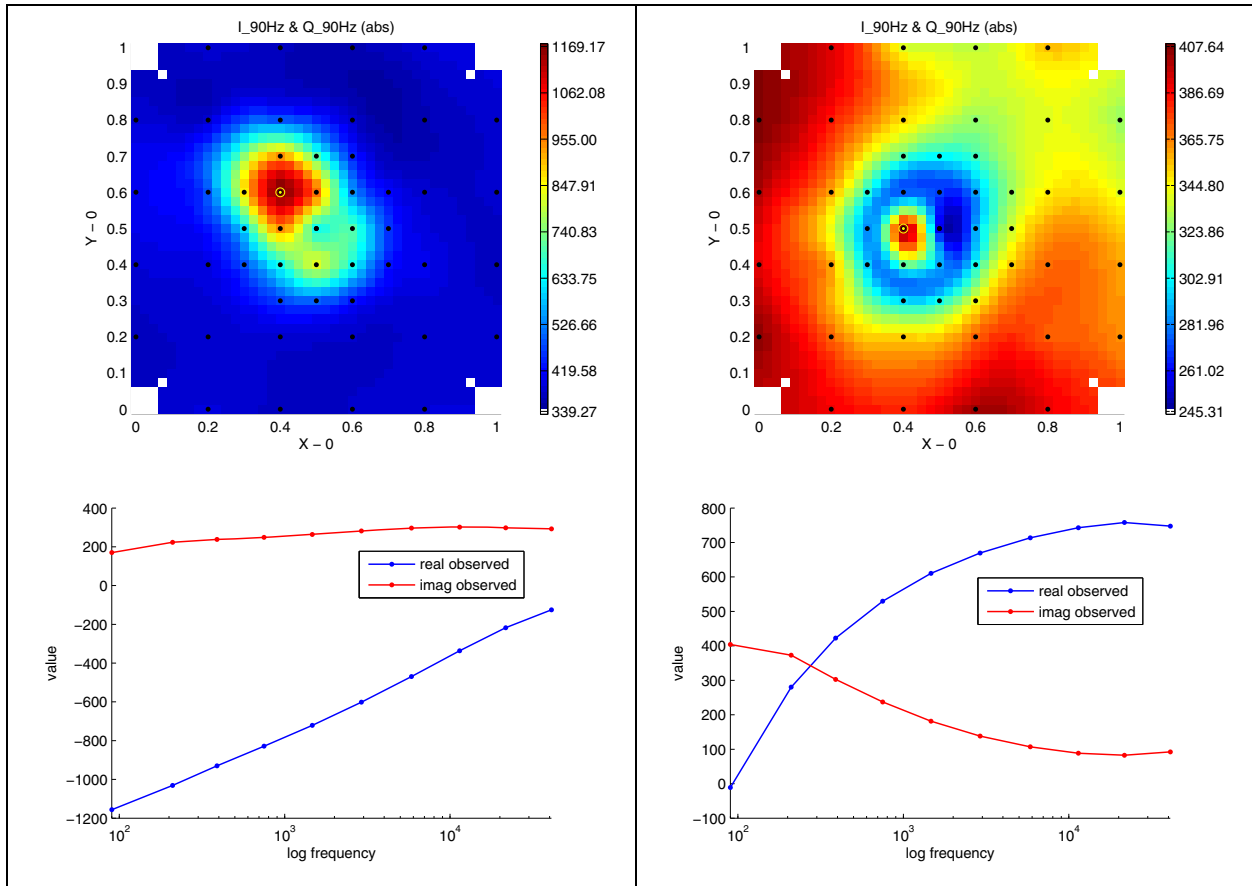
Figure 21. GEM-3 data from a 20-mm projectile buried in cell 56B (left panel) and a 40-mm grenade buried in Cell 64B (right panel) of the Sky Research test plot. Top panels contain a gridded image of the absolute value of the 90-Hertz (Hz) inphase and quadrature data, while the bottom panels illustrate the frequency spectra at a point directly over the target (indicated by the yellow circle on the gridded image). Measurement points are indicated by black dots.

Table 2. Details of location and orientation of ordnance items from selected cells in the Sky Research test plot.

Item	Cell	Depth, cm	Azimuth, °	Dip, °
20-mm M55	56B	5.5	305	0
40-mm M385	64B	11.5	281	10

3.9. Ohio State fully polarimetric GPR cued interrogation

Ohio State University's (OSU) fully polarimetric GPR was initially deployed as part of the field efforts at Camp Lejeune. The results were promising in spite of saturated ground conditions. The extra information gathered in the fully polarimetric measurements allowed for a more sophisticated classification of targets than could be achieved using a COTS GPR system. In order to investigate the OSU system's performance at a

second site under more challenging soil conditions for GPR measure-
ments, the OSU system was deployed at the Ashland test plot. Figure 22
shows the OSU system acquiring data at the Ashland site. Data collection
was focused over multiple-object cells to gauge how effectively the system
could distinguish between potentially overlapping target responses.

Figure 22. Ohio State University's fully polarimetric GPR system acquiring data at the Sky
Research Ashland test plot.

The OSU GPR system collects fully polarimetric backscattered fields from
10 to 810 MHz at 4-MHz increments. At the Ashland test site, a
Schonstedt handheld magnetometer was used to elicit the direction of a
magnetic dipole orientation and to direct the orientation of the GPR
survey lines collected over the target. Collected data were then processed
and late time target features such as natural resonance and polarization
were investigated to differentiate clutter from UXO-like objects. The site
was challenging due to scattering from near-surface layers as well as
scattering from the walls and base of the excavations for the target
emplacements. When the target response dominated the clutter caused by
layer and trench scattering, data were analyzed and late time features
exploited for classification as shown in Figure 23. Further details of the
Ashland measurements and results can be found in Youn and Chen
(2007).
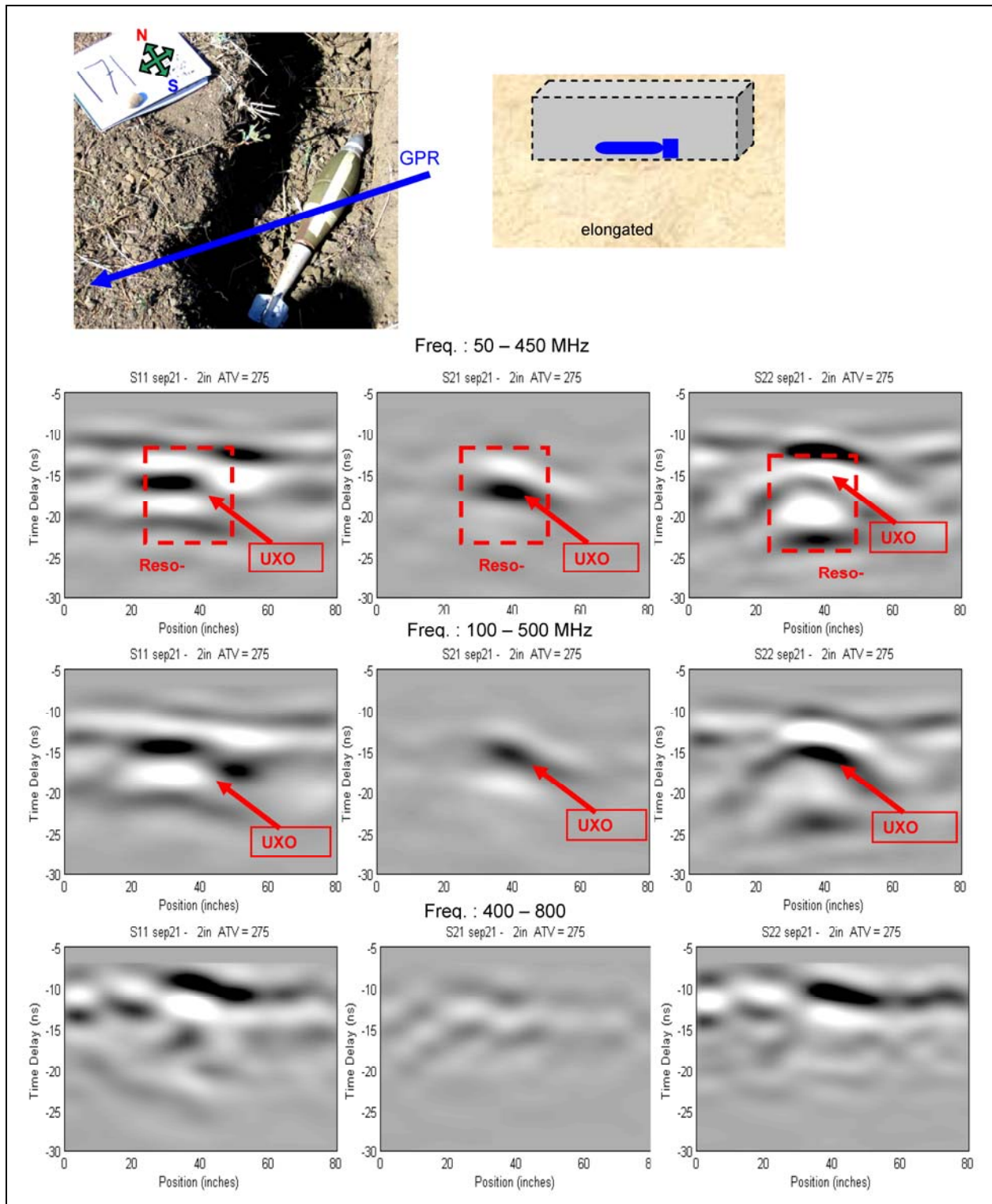
Figure 23. A large, horizontal UXO target produces strong returns, which allow for analysis of late-time features in the data. The results for different frequencies are shown in the different rows, and the results for different polarizations are shown in the columns. The left column (S11) and the right column (S22) are the co-polarization measurements, while the middle column (S21) represents the cross-polarized measurements. The antenna used had two perpendicularly polarized antenna elements. A polarization of 1 refers to the antenna element that was parallel to the direction of travel, while 2 refers to the transverse element.

4 Discussion

The test plot data described in this report were well utilized as the following list of results indicates:

1. A paper was published in the *Journal of Applied Geophysics* that used data acquired at the Ashland test plot to investigate the effect of data quality on time-domain electromagnetic discrimination. Field data from different survey modes were analyzed to identify noise sources and provide quantitative estimates of the noise in each survey. Full details can be found in Walker et al. (2007).

2. A second paper published in the *Journal of Applied Geophysics* successfully tested a library-based method for UXO discrimination. A library of dipole polarization parameters was generated by inverting the high quality data acquired at the ERDC test stand over a set of targets (see Report 3). These same targets surveyed on the test stand were emplaced and surveyed at the Ashland test plot with an EM-63. The observed response for each test plot target was compared with the items from the test stand library to determine which target in the library was most likely to have produced the observed data anomaly. Full details can be found in Pasion et al. (2007).

3. A modified EM-61 cart system (RTS, IMU, suspension cart) was compared to a baseline EM-61 system (GPS and standard cart, refer to Report 5).

4. A modified EM-63 cart system (RTS, IMU, suspension cart) was compared to a baseline EM-63 system (GPS and standard cart, refer to Report 5).

5. Discrimination and cued-interrogation deployments of the EM-63 were compared (refer to Report 5).

6. EM-61 discrimination performance was compared using the standard four time channels and two configurations with three time channels and a vertical difference measurement. Full details can be found in the Billings et al. (2006).

7. Magnetometer discrimination performance was prepared using man-portable and a standard and a gradient cart configuration. Full details can be found in Report 5 and Billings et al. (2006).

8. Ohio State University's fully polarimetric GPR system acquired data over a number of the multi-object scenarios in the Ashland test plot. They were able to test a new antenna design and develop new processing strategies to deal with scattering from near surface layers and trench effects that were

observed at the Ashland site. Full details can be found in Youn and Chen (2007).

References

Billings, S. D., K. Kingdon, and L. P. Pasion. 2006. *3-D geophysical data analysis, Part II, Analysis of magnetometer and EM-61 data from the Ashland test plot.* Technical Report. Ashland, OR: Sky Research, Inc.

Pasion, L. P., S. D. Billings, D. W. Oldenburg, and S. E. Walker. 2007. Application of a library-based method to time domain electromagnetic data for the identification of unexploded ordnance. *Journal of Applied Geophysics* 61:279–291.

Pasion, C., K. Kingdon, and S. D. Billings. 2005. *UXO standardized test site: Soil sampling program.* Technical Report. Ashland, OR: Sky Research, Inc.

Walker, S. E., L. P. Pasion, S. D. Billings, and D. W. Oldenburg. 2007. Investigating the effect of data quality on time domain electromagnetic discrimination. *Journal of Applied Geophysics* 61:254–278.

Youn, H. S., and C. Chen. 2007. *Ashland UXO field measurement/demonstration.* Technical Report. Sky Research Inc.

Appendix A: Images of Discrimination Mode Data Sets Collected Over the Test Plot
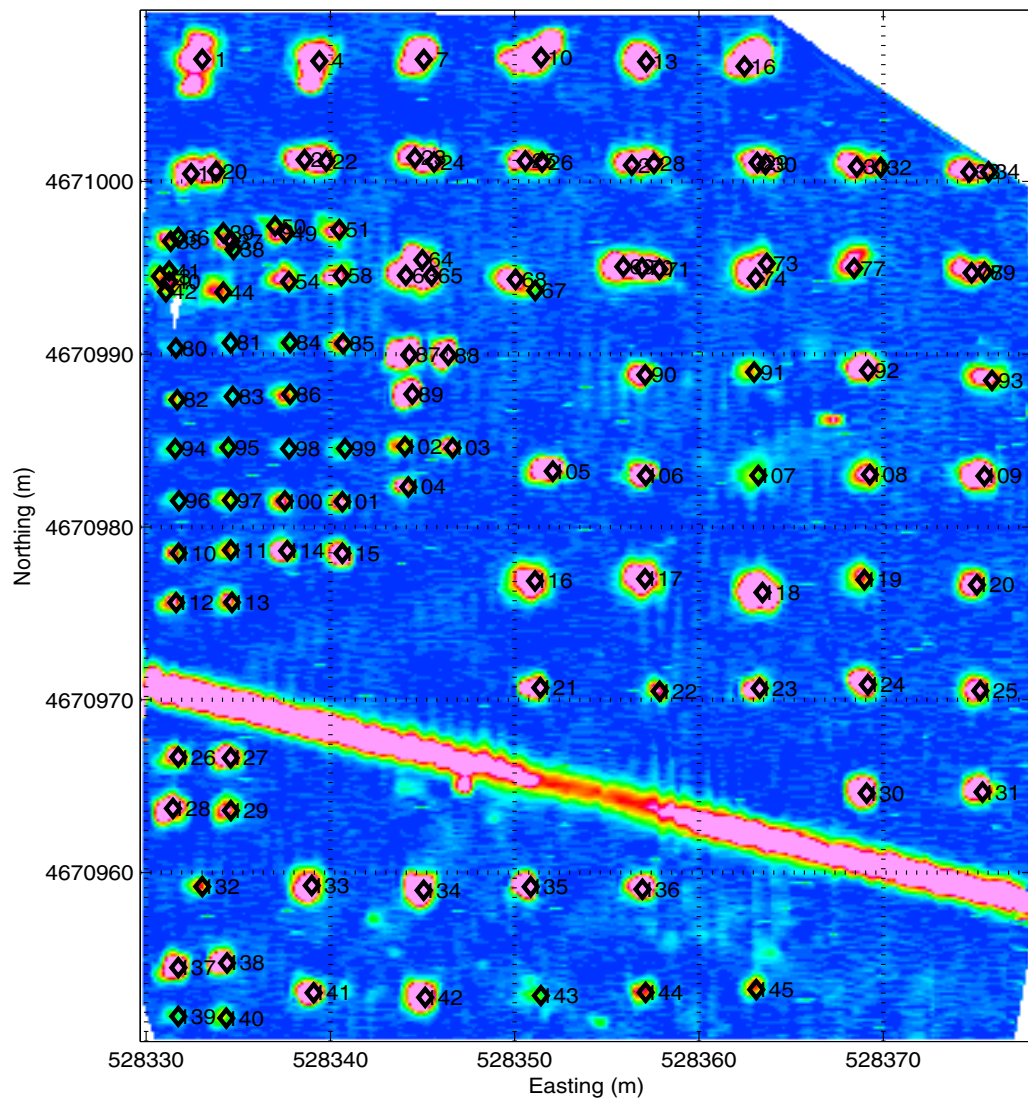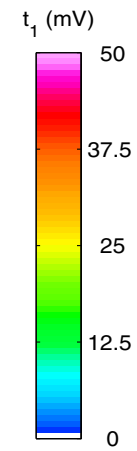
Figure A1. EM-63 cart data collected in September 2005 using a standard cart without an IMU and with GPS for positioning.
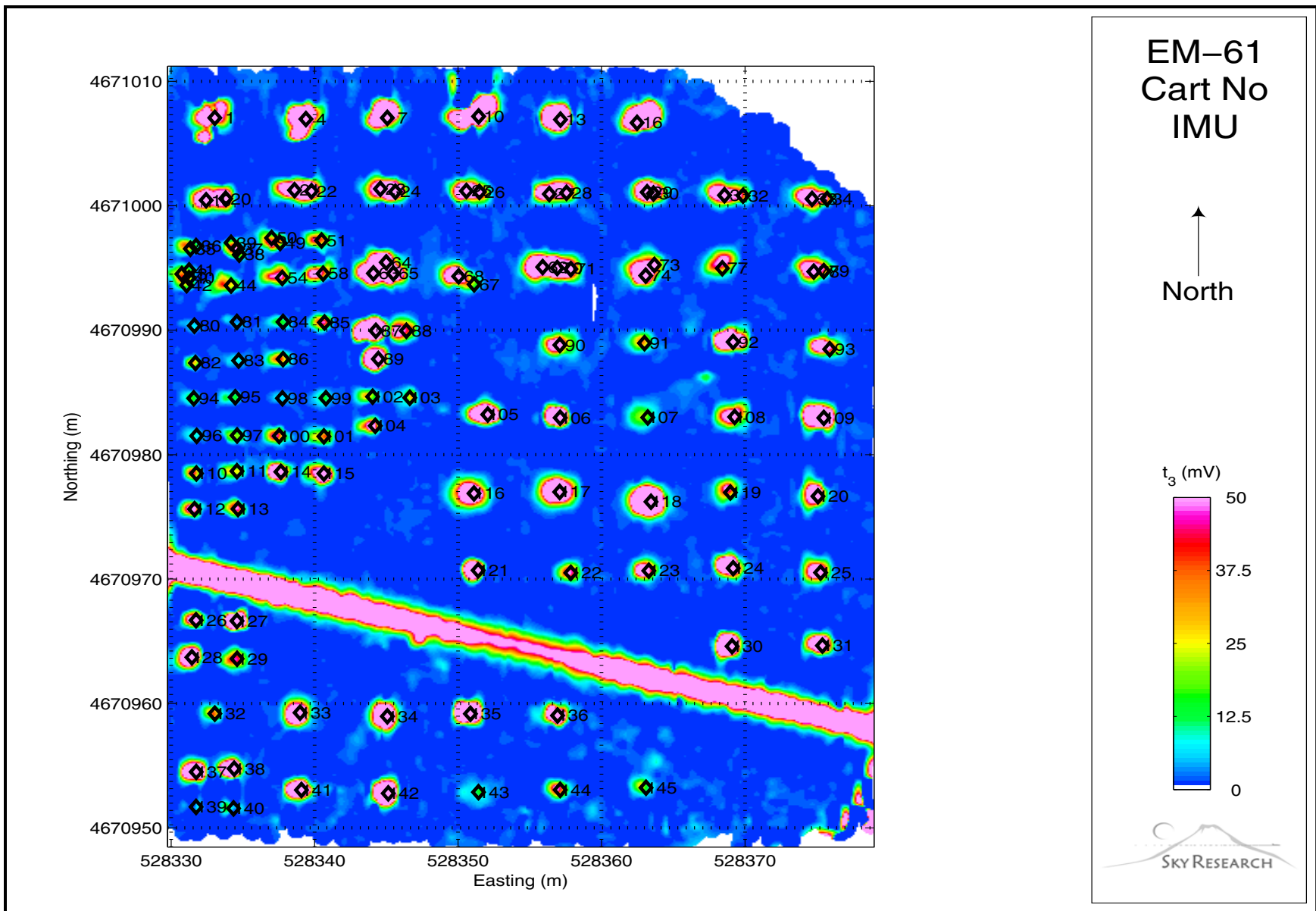
Figure A2. EM-61 cart data collected in September 2005 without an IMU and with GPS for positioning.
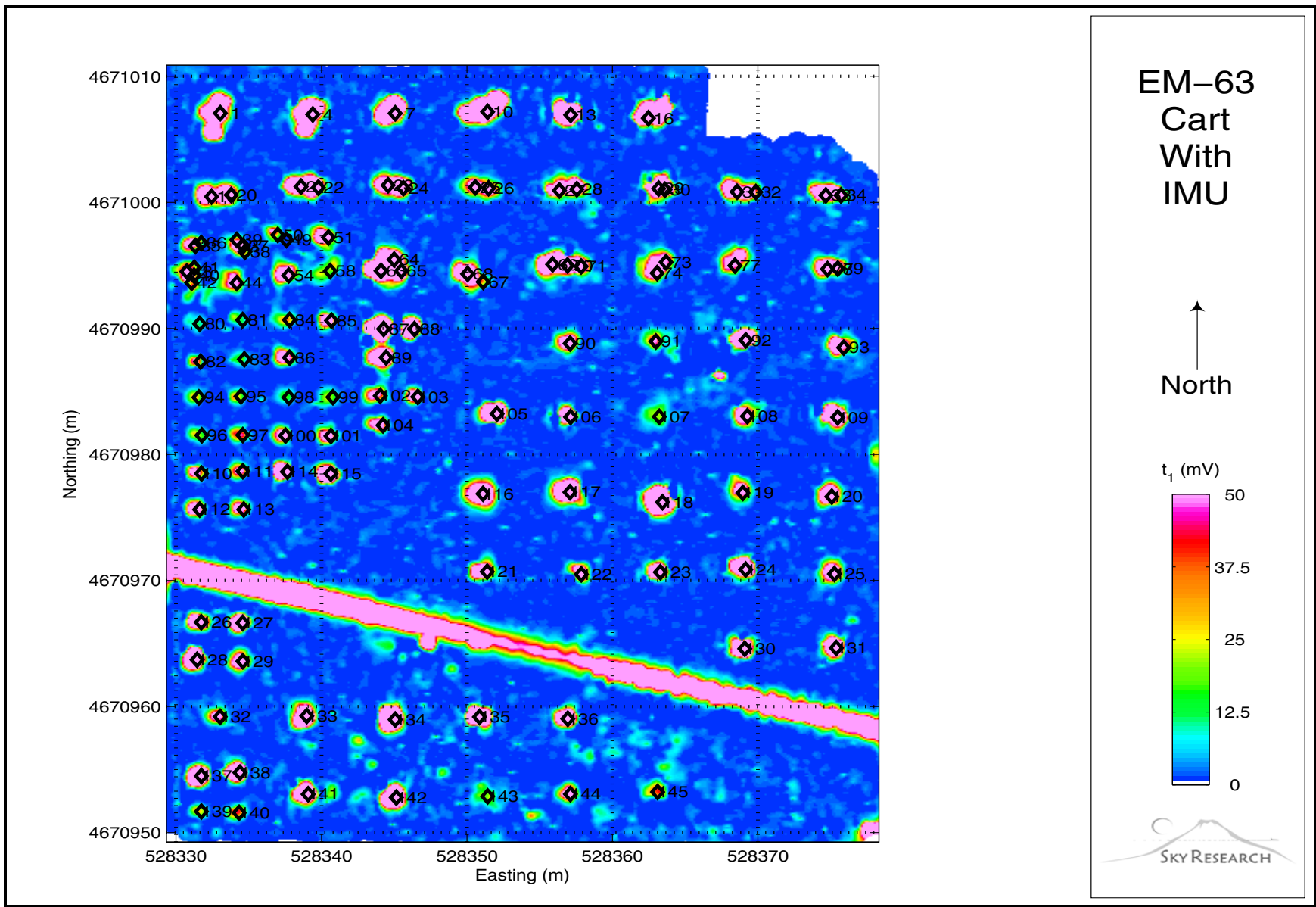
Figure A3. EM-63 suspension cart data collected in February 2006 with an IMU and with RTS for positioning.
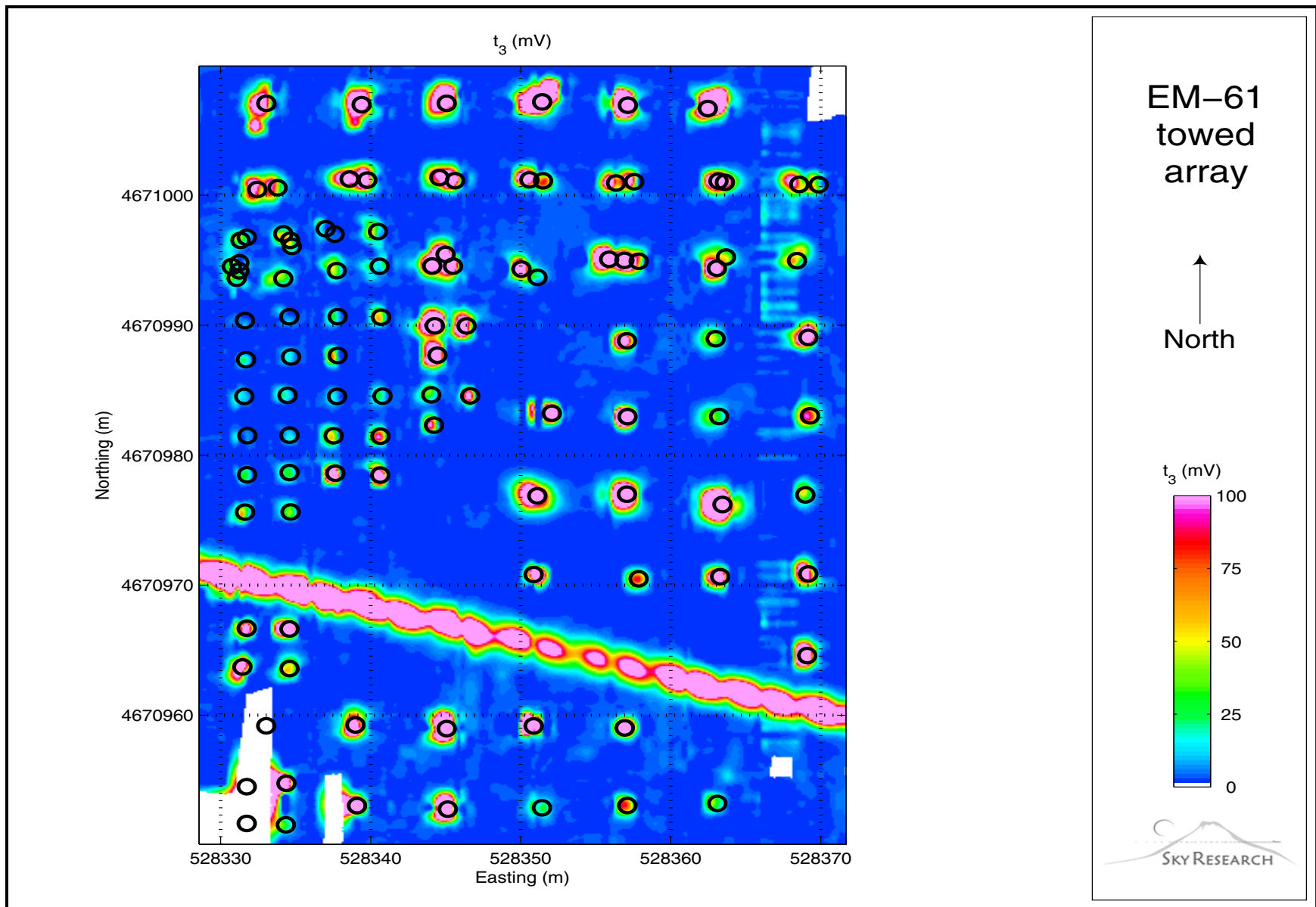
Figure A4. EM-61 towed array data collected over the Ashland test plot in April 2006, with RTS and IMU.

Figure A5. Man-portable magnetometer data collected in May 2006.
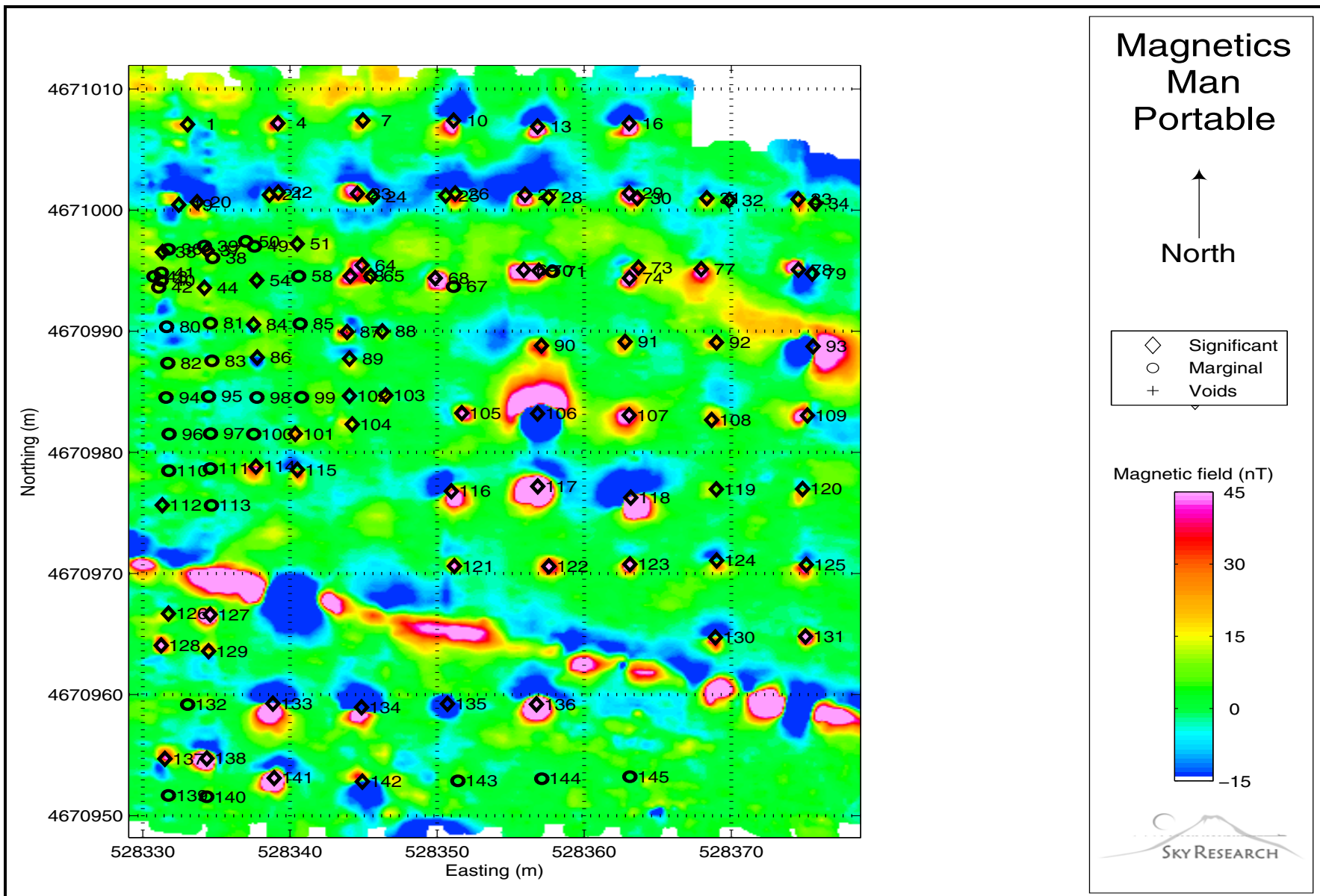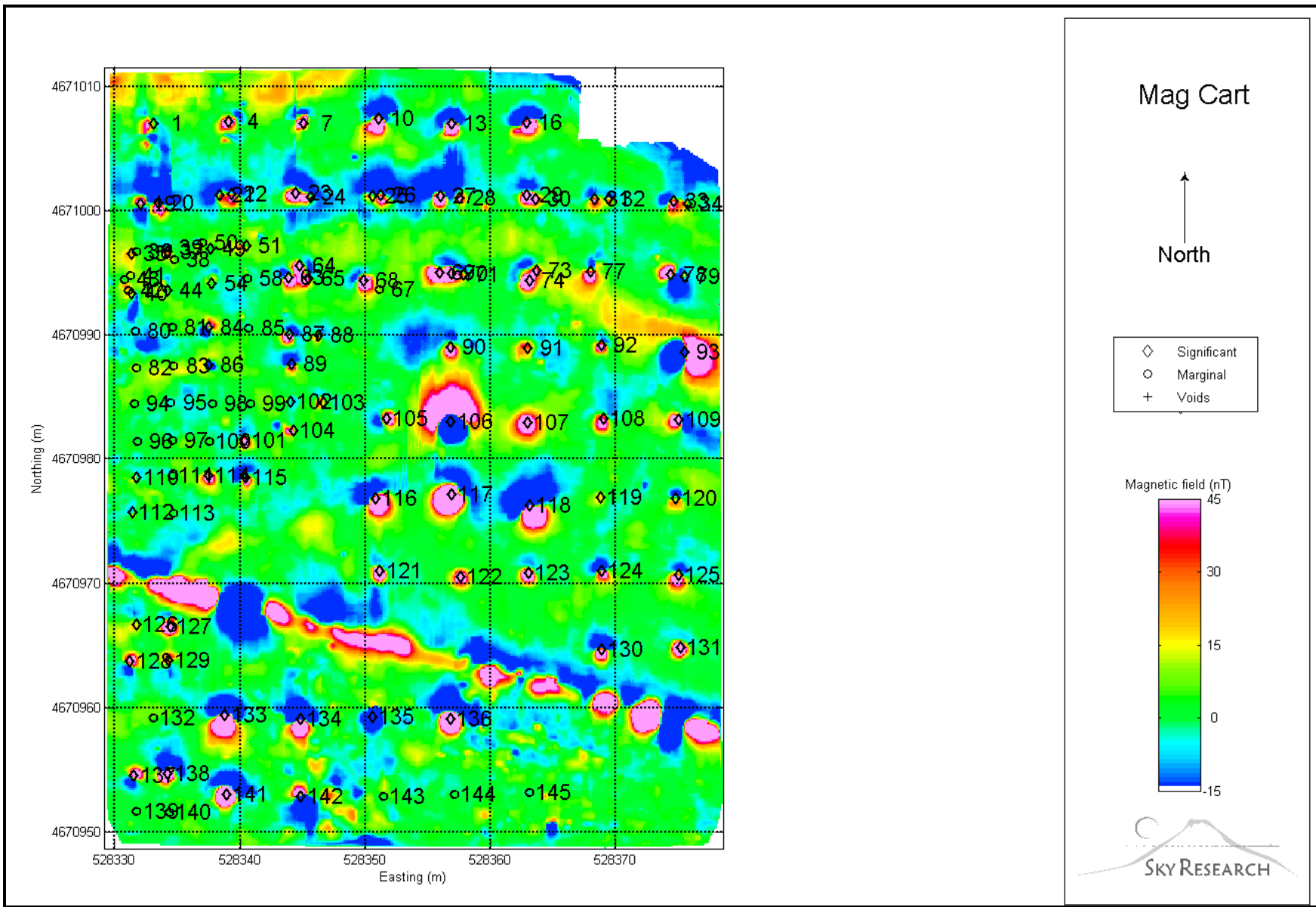
Figure A6. Magnetometer cart data collected in May 2006.
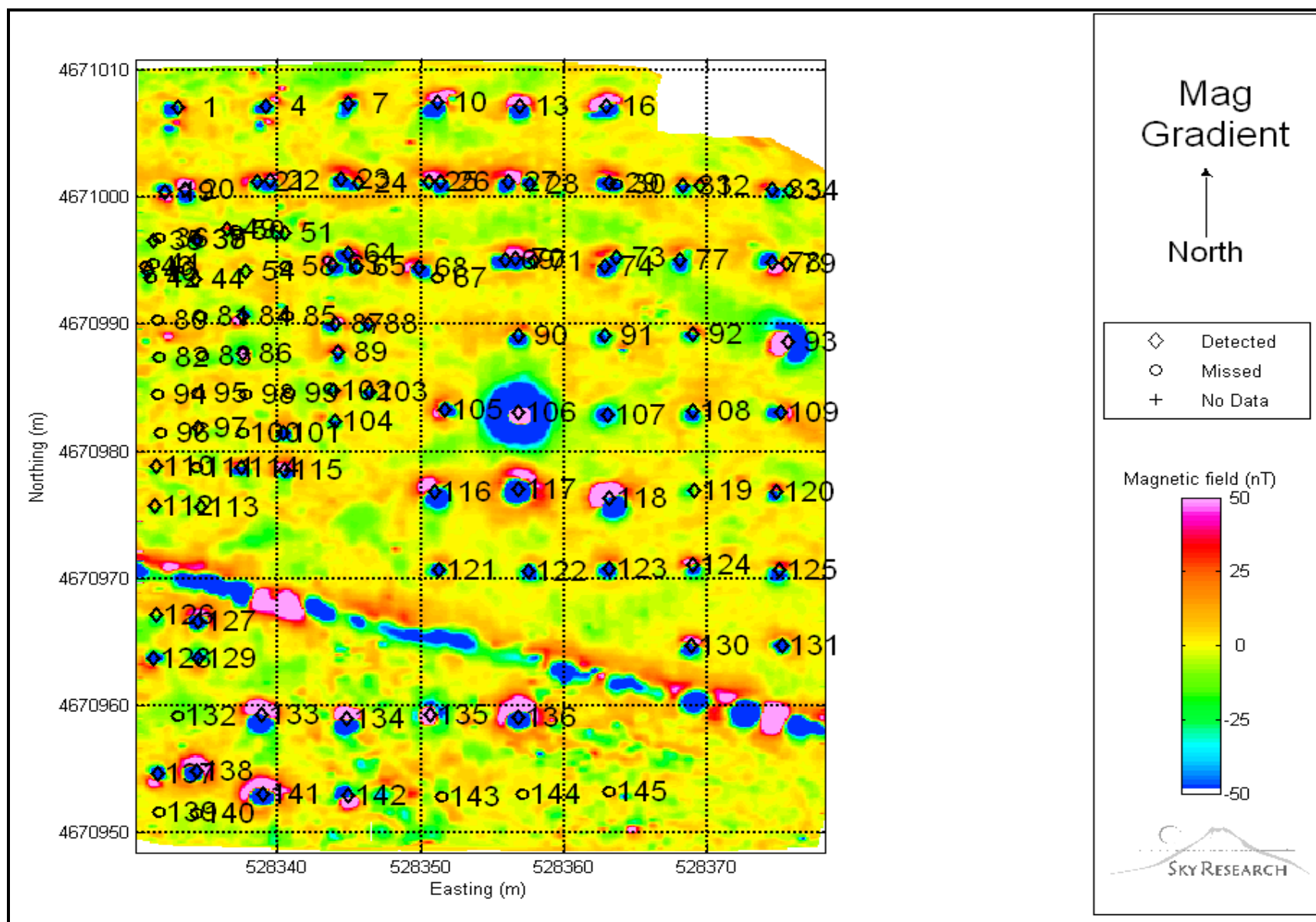
Figure A7. Magnetometer gradient data collected in May 2006.
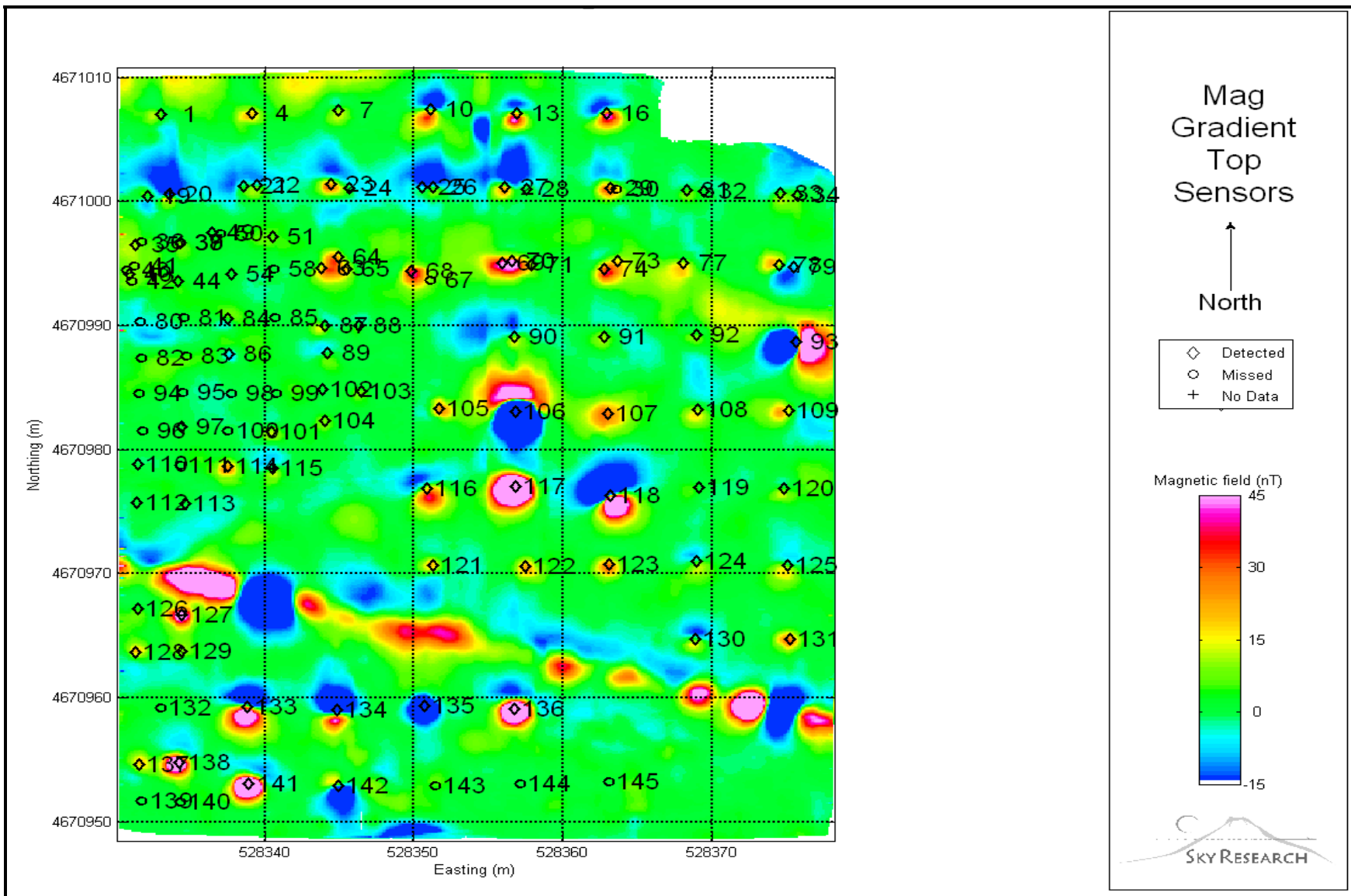
Figure A8. Magnetometer gradient data collected in May 2006 (top sensors)
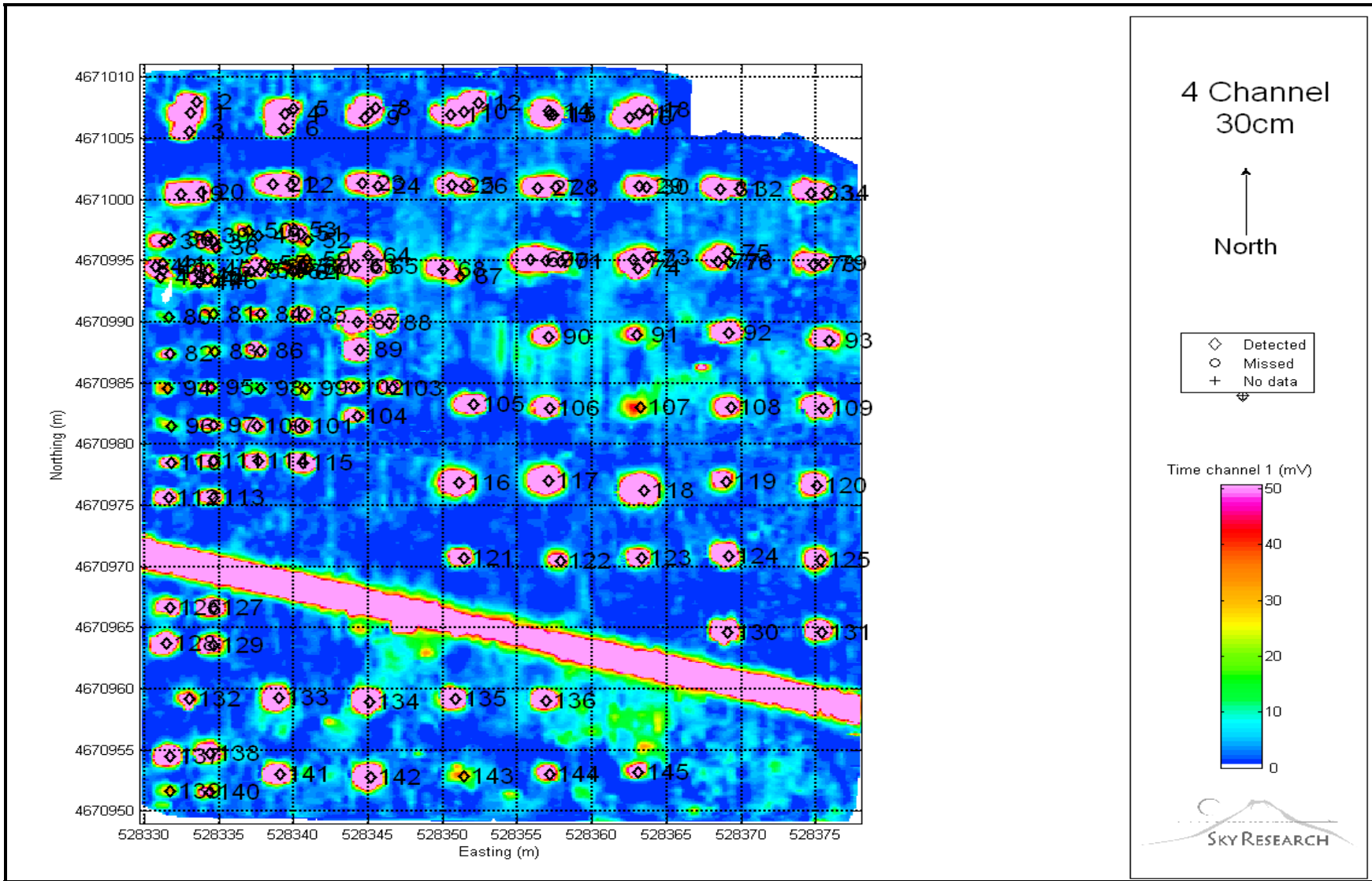
Figure A9. EM-61 cart four-channel data with RTS and IMU collected in May 2006.
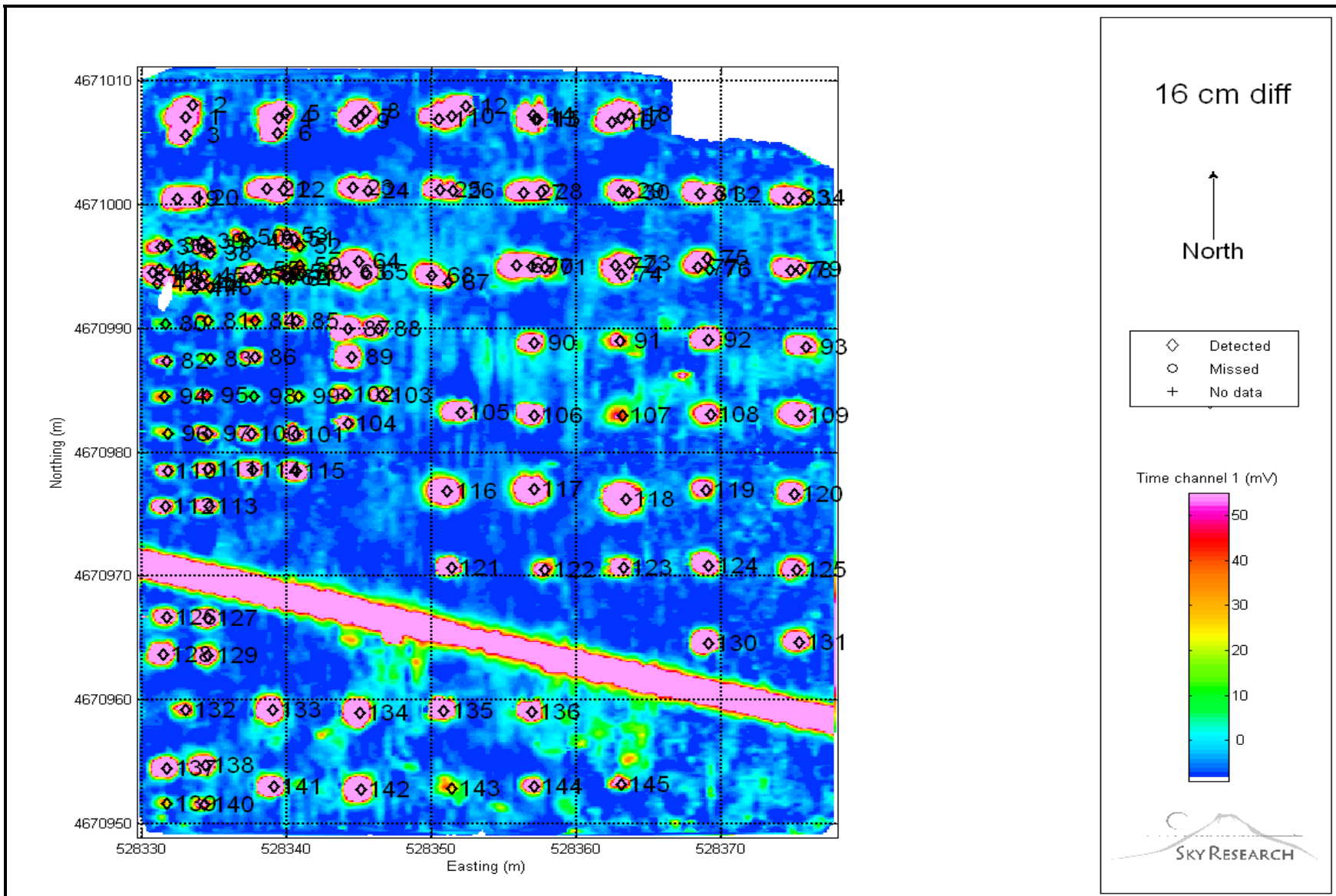
Figure A10. EM-61 cart data collected in May 2006 with top coil 16 cm above bottom coil and with RTS and IMU for positioning.
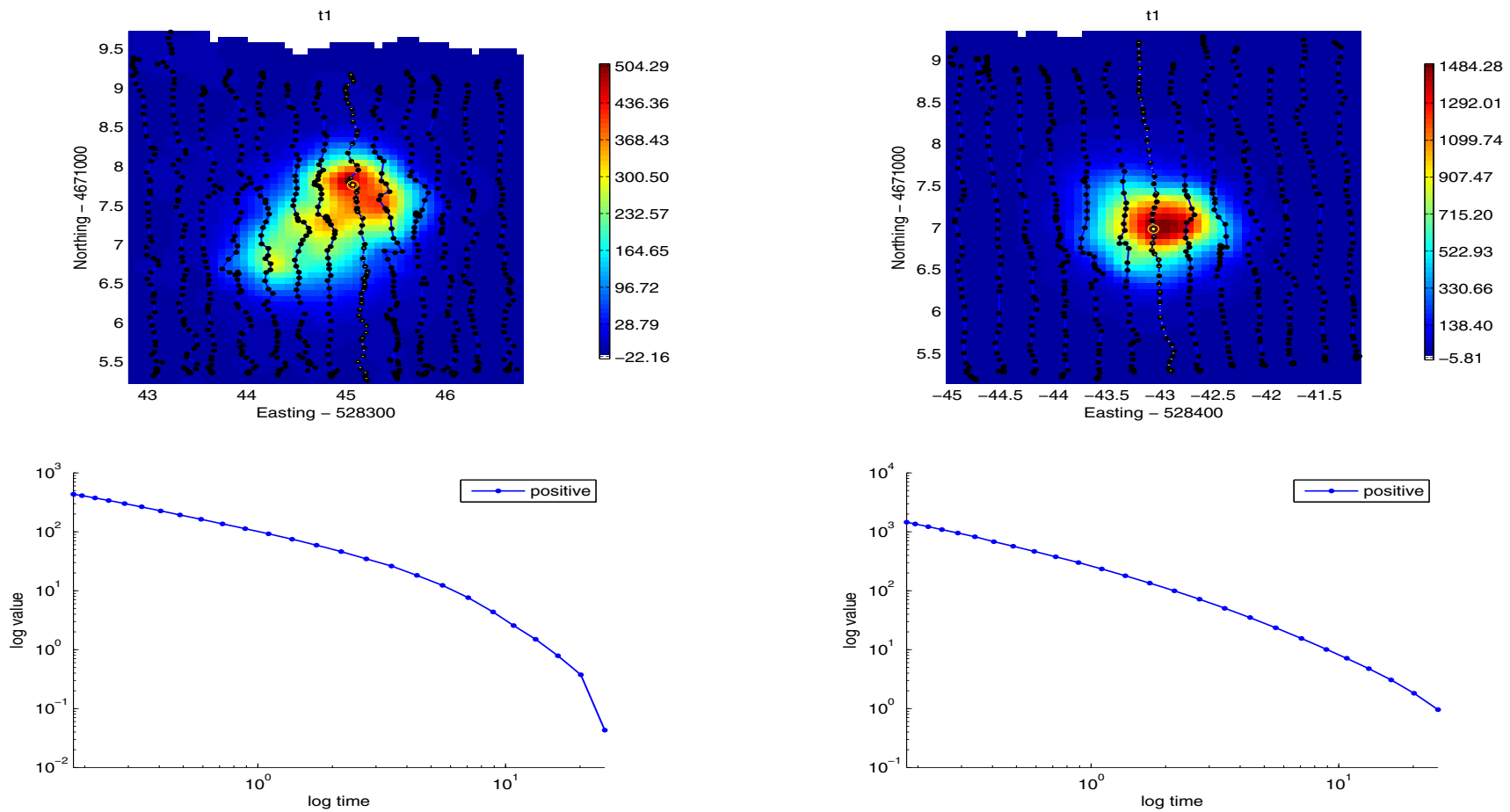
Figure A11. EM-63 cued-interrogation data collected in February 2006 using suspension cart with IMU. Both targets are 105-mm projectiles surrounded by two pieces of shrapnel. Gridded image appears in the top panel and the decay directly over the target (indicated by yellow circle on the gridded image) is shown in the bottom panel.
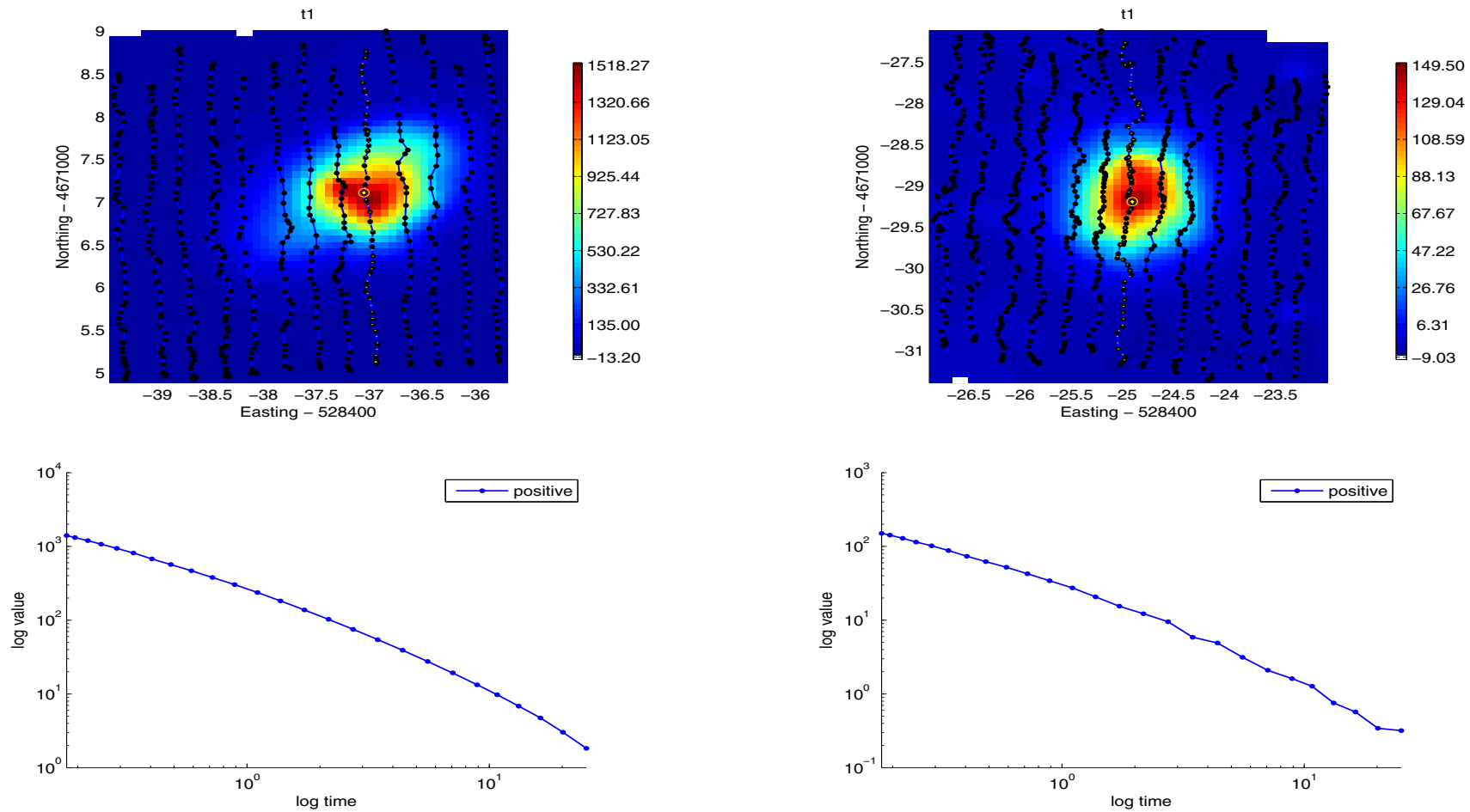
Figure A12. EM-63 cued-interrogation data collected in February 2006 using suspension cart with IMU. Target in the left panel is a 105-mm projectile surrounded by two pieces of shrapnel. The right panel displays data collected over a 90-mm projectile. Gridded image appears in the top panel and the decay directly over the target (indicated by yellow circle on the gridded image) is shown in the bottom panel.
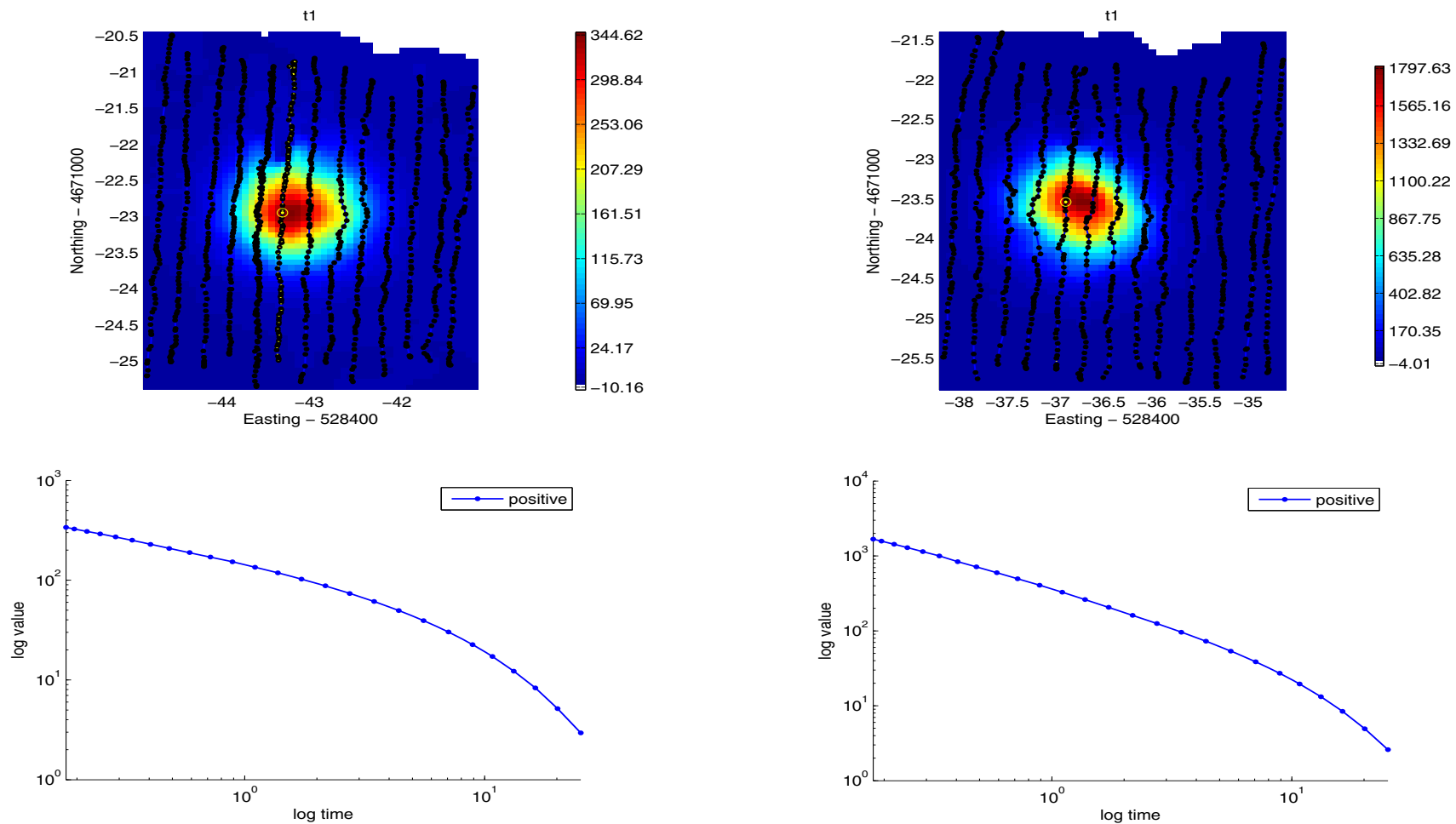
Figure A13. EM-63 cued-interrogation data collected in February 2006 using suspension cart with IMU. Both targets are 155-mm projectiles. Gridded image appears in the top panel and the decay directly over the target (indicated by yellow circle on the gridded image) is shown in the bottom panel.
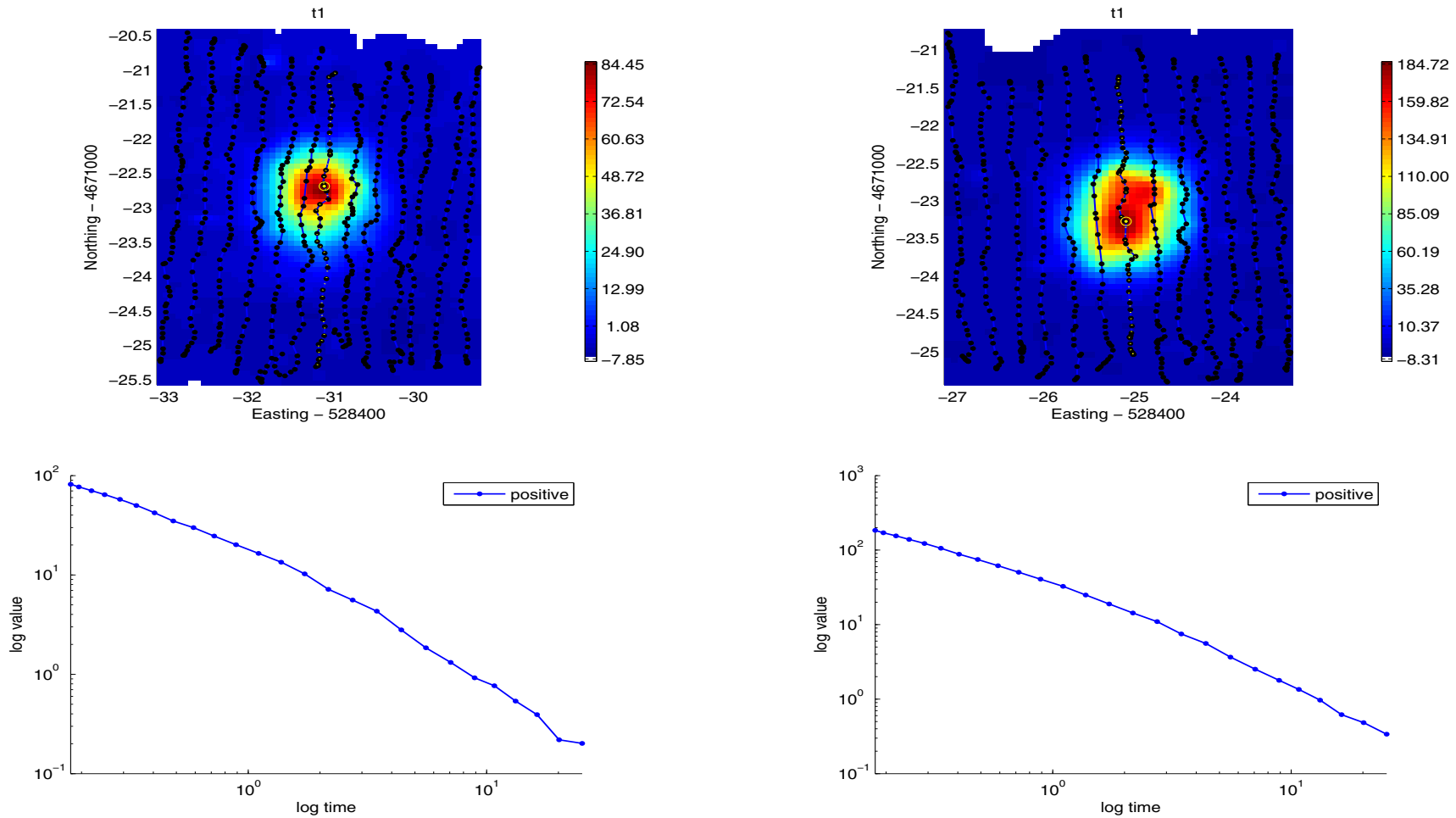
Figure A14. EM-63 cued-interrogation data collected in February 2006 using suspension cart with IMU. Both targets are 76-mm projectiles. Gridded image appears in the top panel and the decay directly over the target (indicated by yellow circle on the gridded image) is shown in the bottom panel.
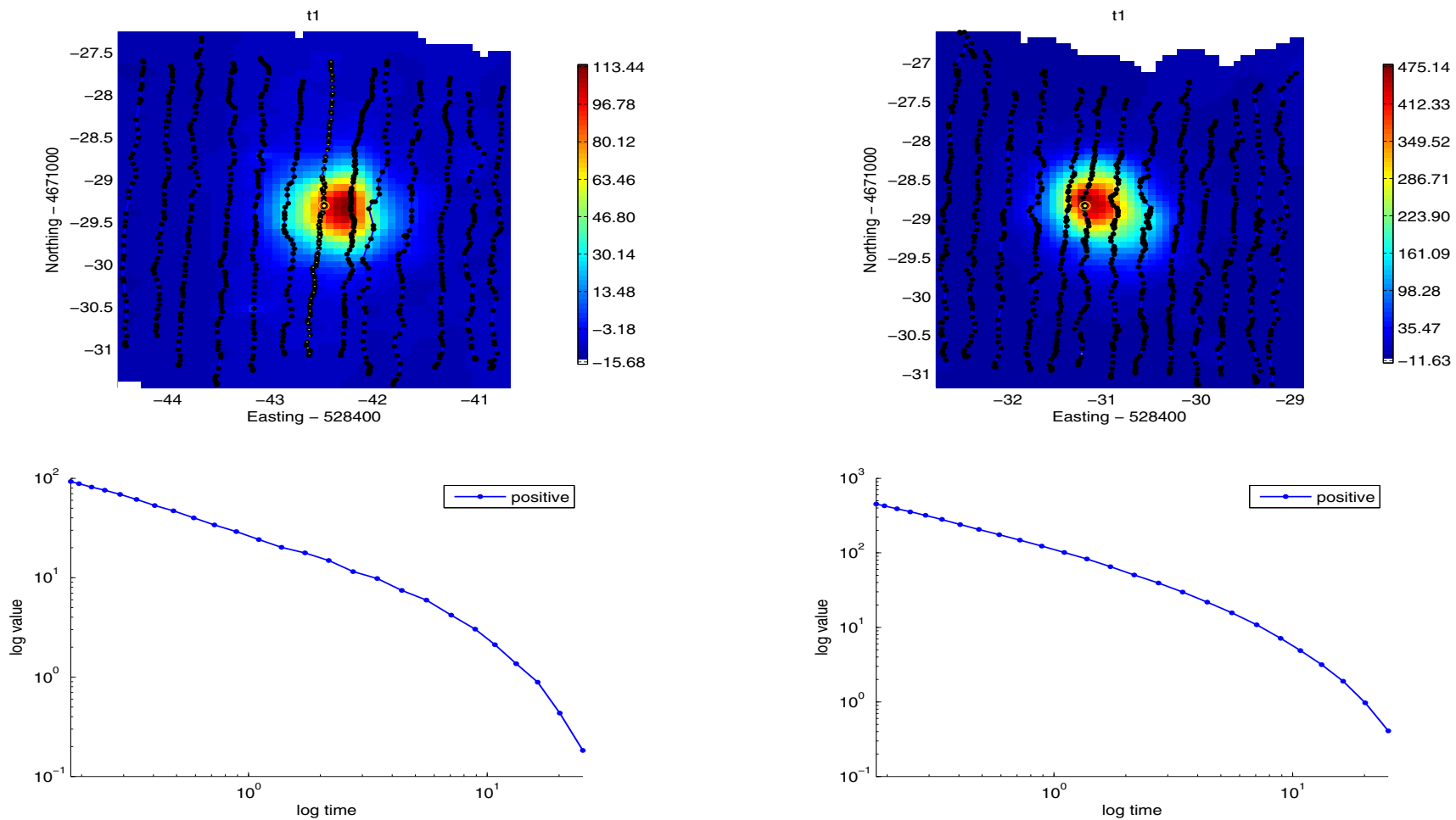
Figure A15. EM-63 cued-interrogation data collected in February 2006 using suspension cart with IMU. Both targets are 81-mm mortars. Gridded image appears in the top panel and the decay directly over the target (indicated by yellow circle on the gridded image) is shown in the bottom panel.

Appendix B: Ashland Test Plot Emplacement Information

Target	Item	Grid Cell	Depth cm	Azimuth °	Dip °	Easting_UTM	Northing_UTM	Elevation m	Origin	Status
Simulant-6-in. steel tubing	S5	93A	21	202	2	528331.7426	4670954.5	575.8347	Ashland metal fabricator	intact
Simulant-6-in. steel tubing	S6	93B	18.5	202	74	528334.3885	4670954.759	575.9672	Ashland metal fabricator	intact
Simulant-6-in. aluminum rod	S7	93C	34	3	65	528331.7413	4670951.679	575.7092	Ashland metal fabricator	intact
Simulant-6-in. aluminum rod	S8	93D	24	3	83	528334.3432	4670951.568	575.8958	Ashland metal fabricator	intact
Simulant-12-in. steel tubing	S14	94	22.5	185	89	528339.0839	4670953.041	576.0853	Ashland metal fabricator	intact
Simulant-12-in. steel tubing	S15	95	21	185	2	528345.1369	4670952.776	576.3297	Ashland metal fabricator	intact
Simulant-12-in. aluminum rod	S16	96	41.5	255	16	528351.4186	4670952.875	576.4837	Ashland metal fabricator	intact
Simulant-12-in. aluminum rod	S17	97	21	255	23	528357.1107	4670953.058	577.0753	Ashland metal fabricator	intact
Simulant-12-in. aluminum rod	S18	98	20	255	89	528363.1042	4670953.223	577.1307	Ashland metal fabricator	intact
Simulant-6-in. aluminum rod	S9	88	21	0	-5	528333.0386	4670959.183	575.865	Ashland metal fabricator	intact
Simulant-12-in. steel rod	S10	89	37	184	-20	528338.9888	4670959.252	576.0166	Ashland metal fabricator	intact
Simulant-12-in. steel rod	S11	90	25	184	-17	528345.0633	4670958.967	576.4066	Ashland metal fabricator	intact
Simulant-12-in. steel rod	S12	91	22	184	96	528350.8649	4670959.174	576.7118	Ashland metal fabricator	intact
Simulant-12-in. steel tubing	S13	92	38	185	88	528356.9325	4670959.027	576.8817	Ashland metal fabricator	intact

Target	Item	Grid Cell	Depth cm	Azimuth °	Dip °	Easting_UTM	Northing_UTM	Elevation m	Origin	Status
Simulant-6-in. steel rod	S1	85A	40.5	28	83	528331.7355	4670966.688	575.8782	Ashland metal fabricator	intact
Simulant-6-in. steel rod	S2	85B	20.5	28	87	528334.5864	4670966.638	576.1082	Ashland metal fabricator	intact
Simulant-6-in. steel rod	S3	85C	23.5	28	10	528331.4509	4670963.711	575.9785	Ashland metal fabricator	intact
Simulant-6-in. steel tubing	S4	85D	40.5	202	9	528334.5911	4670963.592	575.8628	Ashland metal fabricator	intact
Montana 90-mm projectile	MN2-90	86	24	185	0	528369.1003	4670964.594	577.1743	Montana	intact - fired
Montana 90-mm projectile	74	87	27	185	-60	528375.3924	4670964.65	577.4829	Montana	intact - fired
Montana 76-mm projectile	MN1-76	80	21	190	-99	528351.3937	4670970.703	576.8819	Montana	intact - fired
Montana 81-mm mortar	161	81	43	325	-101	528357.8617	4670970.494	576.6787	Montana	intact - fired
Montana 81-mm mortar	153	82	23	325	-73	528363.2948	4670970.663	577.0646	Montana	intact - fired
Montana 81-mm mortar	142	83	223	325	25	528369.1681	4670970.869	577.2609	Montana	intact - fired
Montana 90-mm projectile	MN3-90	84	45	186	7	528375.2696	4670970.52	577.4165	Montana	intact - fired
Montana white phosphorous frag	MN1-F	58A	18	NA	NA	528344.2745	4670989.954	577.0878	Montana	frag - fired
Montana white phosphorous frag	MN2-F	58B	12	NA	NA	528346.3904	4670989.95	577.1985	Montana	frag - fired
Montana white phosphorous frag	MN3-F	58C	13	NA	NA	528344.446	4670987.69	577.092	Montana	frag - fired
37-mm projectile	37mm1	66A	15.5	74	0	528344.039	4670984.652	576.9294	ATC	intact - unfired
37-mm projectile	37mm2	66B	7.5	74	-90	528346.6301	4670984.571	577.0794	ATC	intact - unfired
37-mm projectile	37mm3	66C	7.5	74	-90	528344.2272	4670982.313	576.9626	ATC	intact - unfired
M42 submunition	103	72A	11.5	122	-90	528331.758	4670978.489	576.4831	ATC	intact - unfired
BLU-26 submunition	476	72B	20.5	312	0	528334.588	4670978.665	576.4776	ATC	intact - unfired
BLU-26 submunition	473	72C	11	312	0	528331.6268	4670975.622	576.3643	ATC	intact - unfired
BLU-26 submunition	477	72D	11	312	-21	528334.6588	4670975.631	576.4439	ATC	intact - unfired

Target	Item	Grid Cell	Depth cm	Azimuth °	Dip °	Easting_UTM	Northing_UTM	Elevation m	Origin	Status
60-mm M493A	187	73A	16.5	324	-80	528337.6494	4670978.621	576.6867	ATC	intact - unfired
60-mm M493A	186	73B	17	324	-21	528340.6428	4670978.475	576.7064	ATC	intact - unfired
155-mm M483A1	905	75	71	315	7	528351.1049	4670976.876	576.5442	ATC	intact - unfired
155-mm M483A1	904	76	45	315	-106	528357.0796	4670977.001	577.0087	ATC	intact - unfired
155-mm M483A1	906	77	34.5	315	8	528363.4434	4670976.211	577.1316	ATC	intact - unfired
Montana 76-mm projectile	MN2-76	78	46	190	-20	528368.9768	4670976.95	577.2767	Montana	intact - fired
Montana 76-mm projectile	MN3-76	79	25.5	188	0	528375.0853	4670976.652	577.7394	Montana	intact - fired
40-mm M385	212	64A	13	281	-79	528331.5739	4670984.526	576.6586	ATC	intact - unfired
40-mm M385	137	64B	11.5	281	10	528334.4615	4670984.607	576.7528	ATC	intact - unfired
M42 submunition	001	64C	22	122	15	528331.7794	4670981.511	576.4804	ATC	intact - unfired
M42 submunition	091	64D	10.5	122	15	528334.5913	4670981.542	576.6754	ATC	intact - unfired
MK 118 Rockeye	143	65A	30	248	-107	528337.7576	4670984.527	576.6779	ATC	intact - unfired
MK 118 Rockeye	150	65B	14	248	-94	528340.788	4670984.542	576.7963	ATC	intact - unfired
MK 118 Rockeye	157	65C	14	248	-8	528337.5307	4670981.499	576.7626	ATC	intact - unfired
60-mm M493A	223	65D	32	324	-65	528340.6477	4670981.465	576.6417	ATC	intact - unfired
2.75-in. rocket	809	67	21	269	-21	528352.0716	4670983.225	577.2221	ATC	intact - unfired
2.75-in. rocket	805	68	20	269	-111	528357.1186	4670982.967	577.4265	ATC	intact - unfired
M456 heat rod	901	69	55	286	-100	528363.2195	4670982.984	577.2622	ATC	intact - unfired
M456 heat rod	902	70	30	286	-97	528369.2792	4670983.03	577.677	ATC	intact - unfired
M456 heat rod	72	71	28	286	11	528375.4927	4670982.95	577.9922	ATC	intact - unfired
20mm M55	196	56A	11	305	-20	528331.6213	4670990.361	576.8107	ATC	intact - unfired
20-mm M55	183	56B	5.5	305	0	528334.5855	4670990.66	576.946	ATC	intact - unfired
20-mm M55	194	56C	6	305	-82	528331.6908	4670987.36	576.8003	ATC	intact - unfired

Target	Item	Grid Cell	Depth cm	Azimuth °	Dip °	Easting_UTM	Northing_UTM	Elevation m	Origin	Status
40-mm M385	201	56D	20	281	-102	528334.698	4670987.558	576.7462	ATC	intact - unfired
BDU-28 submunition	181	57A	19	226	3	528337.8001	4670990.665	576.9222	ATC	intact - unfired
BDU-28 submunition	160	57B	9	226	10	528340.6924	4670990.616	577.1271	ATC	intact - unfired
BDU-28 submunition	111	57C	10.5	226	-114	528337.803	4670987.676	576.9925	ATC	intact - unfired
81-mm M374 mortar	091a	60	22	66	-92	528357.0886	4670988.804	577.5574	ATC	intact - unfired
81-mm M374 mortar	193	61	44	66	-119	528362.9938	4670988.959	577.4346	ATC	intact - unfired
81-mm M374 mortar	171	62	19	66	-6	528369.1716	4670989.06	577.9301	ATC	intact - unfired
2.75-in. rocket	806	63	40	270	16	528375.9059	4670988.478	577.9865	ATC	intact - unfired
37-mm projectile	510	48A-1	15	29	30	528331.3332	4670996.536	576.8094	ATC	intact - unfired
20-mm projectile	521	48A-2	7	110	20	528331.7361	4670996.766	576.9166	FLBGR	rusted spent shell
37-mm projectile	511	48B-1	13.5	142	-61	528334.6291	4670996.534	576.9502	ATC	intact - unfired
20-mm projectile	522	48B-2	7.5	142	30	528334.7415	4670996.065	577.0333	FLBGR	rusted spent shell
20-mm projectile	523	48B-3	10	89	-18	528334.1797	4670997.026	576.9631	FLBGR	rusted spent shell
37-mm projectile	512	48C-1	15	8	-20	528331.246	4670994.189	576.8136	ATC	intact - unfired
20-mm projectile	524	48C-2	5	297	18	528331.2509	4670994.81	576.9312	FLBGR	rusted spent shell
20-mm projectile	525	48C-3	8.5	197	24	528331.0748	4670993.616	576.8957	FLBGR	rusted spent shell
20-mm projectile	526	48C-4	6	267	10	528330.7457	4670994.516	576.919	FLBGR	rusted spent shell
37-mm projectile	513	48D-1	19	240	-23	528334.1788	4670993.589	576.8755	ATC	intact - unfired
20-mm projectile	527	48D-2	5.5	235	5	528334.2876	4670994.316	577.0254	FLBGR	rusted spent shell
20-mm projectile	528	48D-3	8.5	47	-23	528334.7221	4670993.277	576.9904	FLBGR	rusted spent shell
20-mm projectile	529	48D-4	7	215	4	528333.6342	4670993.239	576.948	FLBGR	rusted spent shell
20-mm projectile	530	48D-5	7	217	30	528333.7519	4670993.797	576.9699	FLBGR	rusted spent shell
37-mm projectile	514	49A-1	9	234	9	528337.5912	4670997.01	577.0494	ATC	intact - unfired

Target	Item	Grid Cell	Depth cm	Azimuth °	Dip °	Easting_UTM	Northing_UTM	Elevation m	Origin	Status
20-mm projectile	531	49A-2	3.5	159	10	528336.9986	4670997.416	577.0862	FLBGR	rusted spent shell
37-mm projectile	515	49B-1	7.5	250	0	528340.4864	4670997.213	577.1314	ATC	intact - unfired
20-mm projectile	532	49B-2	5.5	17	0	528340.9121	4670996.637	577.1216	FLBGR	rusted spent shell
20-mm projectile	533	49B-3	8	183	-23	528340.0225	4670997.556	577.1425	FLBGR	rusted spent shell
37-mm projectile	516	49C-1	9	145	-6	528337.7434	4670994.201	577.0383	ATC	intact - unfired
20-mm projectile	534	49C-2	6	333	30	528338.0211	4670994.752	577.0678	FLBGR	rusted spent shell
20-mm projectile	535	49C-3	8	134	-20	528338.4097	4670994.445	577.0386	FLBGR	rusted spent shell
20-mm projectile	536	49C-4	6	251	26	528337.161	4670994.132	577.0698	FLBGR	rusted spent shell
37-mm projectile	517	49D-1	7.5	61	-27	528340.5954	4670994.543	577.0703	ATC	intact - unfired
20-mm projectile	537	49D-2	7	59	2	528340.8962	4670995.086	577.1013	FLBGR	rusted spent shell
20-mm projectile	538	49D-3	7	241	-6	528341.0366	4670994.435	577.0801	FLBGR	rusted spent shell
20-mm projectile	539	49D-4	5	199	-26	528340.4299	4670994.017	577.1029	FLBGR	rusted spent shell
20-mm projectile	540	49D-5	6.5	308	12	528339.982	4670994.149	577.0891	FLBGR	rusted spent shell
90-mm projectile	501	50-1	21	144	2	528344.0968	4670994.563	577.0686	Montana	intact - fired
90-mm projectile	504	50-2	24	104	-47	528344.9911	4670995.454	577.1045	Montana	intact - fired
90-mm projectile	502	50-3	21	189	-34	528345.4863	4670994.553	577.1217	Montana	intact - fired
Tree root	550	51-1	24	285	-46	528351.1773	4670995.404	577.2475	Ashland clutter	NA
37-mm projectile	176	51-2	23	63	2	528351.1151	4670993.686	577.2692	ATC	intact - unfired
81-mm mortar	140	51-3	27	285	-35	528350.0439	4670994.326	577.1718	Montana	intact - fired
105-mm projectile	11	52-1	34	25	56	528355.8916	4670995.07	577.4984	Montana	intact - fired
90-mm projectile	503	52-2	22	104	81	528356.9138	4670994.996	577.6738	Montana	intact - fired
81-mm mortar (no tail fins)	147	52-3	25	147	4	528357.8556	4670994.915	577.6896	Montana	missing tail fin

Target	Item	Grid Cell	Depth cm	Azimuth °	Dip °	Easting_UTM	Northing_UTM	Elevation m	Origin	Status
White phosphorous frag (tail fin 81-mm)	167	53-1	14	NA	NA	528362.7296	4670995.073	577.8245	Montana	frag - fired
76-mm projectile	541	53-2	34	326	-24	528363.6863	4670995.25	577.6328	Montana	intact - fired
81-mm mortar	149	53-3	26	300	-35	528363.0766	4670994.381	577.6708	Montana	blown out - fired
White phosphorous frag	112	54-1	22	NA	NA	528369.0485	4670995.643	577.9658	Montana	intact - fired
Rock	551	54-2	17	NA	NA	528369.2348	4670994.817	578.0285	Ashland clutter	NA
90-mm projectile	542	54-3	50	7	-31	528368.4212	4670994.975	577.6952	Montana	intact - fired
81-mm mortar	159	55-1	35	130	-5	528374.7921	4670994.707	578.0898	Montana	intact - fired
37-mm projectile	520	55-2	12	35	5	528375.4988	4670994.748	578.3527	ATC	intact - unfired
81-mm mortar	505	29-1	30	179	0	528332.443	4671000.45	576.7753	Montana	intact - fired
81-mm mortar	128	29-2	31	2	-4	528333.7965	4671000.578	576.8303	Montana	intact - fired
81-mm mortar	162	30-1	30	275	0	528338.5962	4671001.253	576.9795	Montana	blown out - fired
81-mm mortar	138	30-2	30	183	0	528339.7783	4671001.171	577.0137	Montana	intact - fired
90-mm projectile	503a	31-1	30	100	-90	528344.5841	4671001.36	577.0224	Montana	intact - fired
90-mm projectile	500	31-2	30	100	0	528345.6283	4671001.123	577.1408	Montana	intact - fired
81-mm mortar	137a	32-1	30	27	-90	528350.5789	4671001.189	577.2978	Montana	intact - fired
81-mm mortar	164	32-2	30	286	-90	528351.486	4671001.119	577.2963	Montana	blown out - fired
81-mm mortar	145	33-1	30	27	-90	528356.3595	4671000.943	577.5483	Montana	intact - fired
81-mm mortar	127	33-2	30	263	0	528357.5596	4671001.04	577.6226	Montana	intact - fired
81-mm mortar	126	34-1	31	149	-90	528363.1751	4671001.091	577.8383	Montana	intact - fired
81-mm mortar	154	34-2	30	270	-3	528363.6135	4671000.99	577.8411	Montana	intact - fired
81-mm mortar	160a	35-1	28.5	322	0	528368.5694	4671000.841	577.9088	Montana	intact - fired
37-mm projectile	518	35-2	9	7	-10	528369.8609	4671000.815	578.1403	ATC	intact - unfired

Target	Item	Grid Cell	Depth cm	Azimuth °	Dip °	Easting_UTM	Northing_UTM	Elevation m	Origin	Status
81-mm mortar	150	36-1	30	305	10	528374.6776	4671000.55	578.1372	Montana	intact - fired
37-mm projectile	519	36-2	10	326	5	528375.7171	4671000.55	578.3782	ATC	intact - unfired
105-mm projectile	5	12–1	45	275	0	528333.0424	4671007.073	576.6965	Montana	frag - fired
White phosphorous frag	168	12–2	10.5	NA	NA	528333.5099	4671008.021	577.0529	Montana	frag - fired
White phosphorous frag	35	12–3	17	NA	NA	528333.0069	4671005.589	576.9781	Montana	frag - fired
105-mm projectile	4	13–1	43	174	-27	528339.3959	4671006.974	576.8956	Montana	intact - fired
White phosphorous frag	15	13–2	19.5	NA	NA	528339.9436	4671007.382	577.1249	Montana	frag - fired
White phosphorous frag	106	13–3	11.5	NA	NA	528339.3126	4671005.772	577.2039	Montana	frag - fired
105-mm projectile	10	14–1	50	175	-16	528345.0657	4671007.069	576.8847	Montana	intact - fired
White phosphorous frag	19	14–2	12.5	NA	NA	528345.4699	4671007.522	577.3145	Montana	frag - fired
White phosphorous frag	166	14–3	9.5	NA	NA	528344.7309	4671006.706	577.292	Montana	frag - fired
105-mm projectile	8	15–1	29	21	5	528351.428	4671007.182	577.2996	Montana	intact - fired
White phosphorous frag	20	15–2	16.5	NA	NA	528350.4944	4671006.89	577.3896	Montana	frag - fired
White phosphorous frag	64	15–3	9	NA	NA	528352.3865	4671007.92	577.5619	Montana	frag - fired
105-mm projectile	2	16–1	25	167	-4	528357.1349	4671006.932	577.5637	Montana	intact - fired
White phosphorous frag	60	16–2	10	NA	NA	528357.0314	4671007.224	577.6163	Montana	frag - fired
White phosphorous frag	94	16–3	20	NA	NA	528357.3737	4671006.94	577.7153	Montana	frag - fired
105-mm projectile	506	17–1	25	290	-11	528362.4733	4671006.667	577.8958	Montana	intact - fired
White phosphorous frag	16	17–2	10	NA	NA	528363.1296	4671006.994	577.9129	Montana	frag - fired
White phosphorous frag	19a	17–3	20	NA	NA	528363.6878	4671007.326	578.0156	Montana	frag - fired
105-mm	G1A	old test plot	15	85	0	528320.9594	4670993.102	576.4275	Montana	intact - fired
White phosphorous frag x 2	G1B	old test plot	13.5	NA	NA	528320.9503	4670995.135	576.4952	Montana	frag - fired

Target	Item	Grid Cell	Depth cm	Azimuth °	Dip °	Easting_UTM	Northing_UTM	Elevation m	Origin	Status
Rocks	G1C	old test plot	15	NA	NA	528320.946	4670997.201	576.4822	Ashland clutter	NA
Tree roots	G1D	old test plot	13	NA	NA	528320.9024	4670999.099	576.5079	Ashland clutter	NA
Styrofoam cylinder	G1E	old test plot	12	NA	NA	528320.7613	4671001.014	576.6124	Ashland hardware store	intact
105-mm	G2A	old test plot	34	89	4	528324.3652	4670992.998	576.3599	Montana	intact - fired
White phosphorous frag x 2	G2B	old test plot	31	NA	NA	528324.3129	4670995.084	576.4931	Montana	frag - fired
Rocks	G2C	old test plot	34	NA	NA	528324.3753	4670997.154	576.4379	Ashland clutter	NA
Tree roots	G2D	old test plot	34	NA	NA	528324.2633	4670999.159	576.4104	Ashland clutter	NA
Styrofoam cylinder	G2E	old test plot	28	NA	NA	528324.1075	4671001.056	576.5379	Ashland hardware store	intact
105-mm	G3A	old test plot	43	84	0	528327.1828	4670992.979	576.4008	Montana	intact - fired
White phosphorous frag x 2	G3B	old test plot	43	NA	NA	528327.0688	4670995.086	576.502	Montana	frag - fired
Rocks	G3C	old test plot	41	NA	NA	528326.6307	4670997.006	576.4575	Ashland clutter	NA
Tree roots	G3D	old test plot	44	NA	NA	528326.8186	4670999.06	576.4234	Ashland clutter	NA
Styrofoam cylinder	G3E	old test plot	40	NA	NA	528326.5002	4671001.243	576.4381	Ashland hardware store	intact

REPORT DOCUMENTATION PAGE

Form Approved
OMB No. 0704-0188

1. REPORT DATE *(DD-MM-YYYY)*	2. REPORT TYPE	3. DATES COVERED *(From - To)*
September 2008	Report 4 of 9	

4. TITLE AND SUBTITLE

UXO Characterization: Comparing Cued Surveying to Standard Detection and Discrimination Approaches: Report 4 of 9 – UXO Characterization Using Magnetic, Electromagnetic, and Ground Penetrating Radar Measurements at the Sky Research Test Plot

5a. CONTRACT NUMBER

5b. GRANT NUMBER

5c. PROGRAM ELEMENT NUMBER

6. AUTHOR(S)

Stephen D. Billings, Leonard R. Pasion, Kevin Kingdon, and Jon Jacobson

5d. PROJECT NUMBER
W912HZ-04-C-0039

5e. TASK NUMBER

5f. WORK UNIT NUMBER

7. PERFORMING ORGANIZATION NAME(S) AND ADDRESS(ES)

Sky Research, Inc.
445 Dead Indian Memorial Road
Ashland, OR 97520-9706

8. PERFORMING ORGANIZATION REPORT NUMBER

ERDC/EL TR-08-35

9. SPONSORING / MONITORING AGENCY NAME(S) AND ADDRESS(ES)

Headquarters, U.S. Army Corps of Engineers
Washington, DC 20314-1000;
U.S. Army Engineer Research and Development Center
Environmental Laboratory
3909 Halls Ferry Road, Vicksburg, MS 39180-6199

10. SPONSOR/MONITOR'S ACRONYM(S)

11. SPONSOR/MONITOR'S REPORT NUMBER(S)

12. DISTRIBUTION / AVAILABILITY STATEMENT

Approved for public release; distribution is unlimited.

13. SUPPLEMENTARY NOTES

14. ABSTRACT

A test plot was established close to Sky Research's corporate headquarters in Ashland, Oregon. A comprehensive character-ization of the site prior to emplacement of the ordnance was undertaken to gain an understanding of how the local soils would impact geophysical measurements. Conductivity and susceptibility measurements were made and soil samples were collected for laboratory analysis. Reconnaissance ground penetrating radar (GPR) surveys were conducted to investigate the penetration depths that could be expected and to characterize typical target responses. Penetration depths of approximately 1.0, 0.6, and 0.4 m were achieved using frequencies of 250, 500 and 1000 MHz, respectively. These measurements indicated that the Ashland test plot represented a challenging, yet realistic site in terms of its suitability for GPR measurements. The test plot was used to test modifications to equipment, new cued-interrogation strategies, and modeling methods. Data were collected with a wide range of sensors including time-domain electromagnetics (Geonics EM-61 and EM-63, the Zonge Bird-Cage), frequency domain electromagnetics (Geophex GEM-3), total-field magnetometers (Geometrics cesium vapor G-823 sensors) and ground penetrating radar (Sensors and Software Smart-Cart, Ohio State University fully polarmetric GPR). Various discrimination mode surveys including towed-array, cart-based and man-portable, and cued-interrogation strategies were tested on the site.

15. SUBJECT TERMS

EMI sensors	Ground penetrating radar	Unexploded ordnance (UXO)
Frequency-domain electromagnetic induction (FEM)	Time-domain electromagnetic induction (TEM)	UXO discrimination
	Total-field magnetics	

16. SECURITY CLASSIFICATION OF:

a. REPORT	b. ABSTRACT	c. THIS PAGE	17. LIMITATION OF ABSTRACT	18. NUMBER OF PAGES	19a. NAME OF RESPONSIBLE PERSON
UNCLASSIFIED	UNCLASSIFIED	UNCLASSIFIED		67	19b. TELEPHONE NUMBER *(include area code)*

Standard Form 298 (Rev. 8-98)
Prescribed by ANSI Std. 239.18